remote sensing

Article

Effects of Precipitation and Fire on Land Surface Phenology in the Brazilian Savannas (Cerrado)

Monique Calderaro da Rocha Santos [1], Lênio Soares Galvão [2,*], Thales Sehn Korting [2] and Grazieli Rodigheri [1]

[1] Remote Sensing Postgraduate Program (PGSER), Coordination for Education, Research and Outreach (COEPE), National Institute for Space Research (INPE), Avenida dos Astronautas, 1758, Jardim da Granja, São José dos Campos 12227-010, SP, Brazil; monique.santos@inpe.br (M.C.d.R.S.); grazieli.rodigheri@inpe.br (G.R.)

[2] Remote Sensing Postgraduate Program (PGSER), National Institute for Space Research (INPE), Earth Observation and Geoinformatics Division (DIOTG), Earth Sciences General Coordination (CGCT), Avenida dos Astronautas, 1758, Jardim da Granja, São José dos Campos 12227-010, SP, Brazil; thales.koerting@inpe.br

* Correspondence: lenio.galvao@inpe.br

Abstract: In protected areas of the Brazilian savannas (Cerrado), Land Surface Phenology (LSP) is influenced by both precipitation and fire, but the nature of these relationships remains unexplored. Here, we assessed the impacts of precipitation and fire on LSP metrics derived from the Normalized Difference Vegetation Index (NDVI) at Emas National Park (ENP). Using TIMESAT, along with the 250-m Moderate Resolution Imaging Spectroradiometer (MODIS) MOD13Q1 and 30-m Harmonized Landsat Sentinel (HLS) products, we investigated these effects in both grassland and woodland areas. To evaluate the effects of precipitation, we identified the driest and wettest seasonal cycles between 2002 and 2023 and analyzed the relationships between accumulated rainfall during the rainy season and each of the 13 TIMESAT metrics. To assess the effects of fire, three major events were examined: 1 September 2005 (affecting 45% of the park's area), 12 August 2010 (90%), and 10 July 2021 (21%). The burned grassland area and the subsequent vegetation recovery following the 2021 event were analyzed in detail using a non-burned control site and LSP metrics extracted from the HLS product, covering both pre- and post-disturbance cycles. The results indicated that the metrics most positively correlated to precipitation were Amplitude (AMP), End of Season (EOS), Large and Small Seasonal Integrals (LSI and SSI), and Rate of Increase at the Beginning of the Season (RIBS). The highest correlation coefficients were found in woodland areas, which were less affected by fire disturbance than grassland areas. Similar trends were observed in the behavior of AMP, EOS, and SSI in response to both precipitation and fire, with fire exerting a stronger influence. By decoupling the fire effects from rainfall influence using the control site, we identified Base Level (BL), SSI, EOS, AMP, and Values at the End and Start of the Season (VES and VSS), as the metrics most sensitive to fire and subsequent vegetation recovery in burned areas. The effects of fire were evident for most metrics, both during the disturbance cycle and in the post-fire cycle. Our study underscores the importance of combining MODIS and HLS time series to understand vegetation phenology in the Cerrado.

Keywords: Cerrado; vegetation phenology; time series; HLS; burned areas; TIMESAT

Academic Editor: Brenden E. McNeil

Received: 1 May 2025
Revised: 9 June 2025
Accepted: 14 June 2025
Published: 17 June 2025

Citation: Santos, M.C.d.R.; Galvão, L.S.; Korting, T.S.; Rodigheri, G. Effects of Precipitation and Fire on Land Surface Phenology in the Brazilian Savannas (Cerrado). *Remote Sens.* **2025**, *17*, 2077. https://doi.org/10.3390/rs17122077

1. Introduction

The Cerrado, a tropical savanna in Brazil, is the second largest biome in the country, covering 2,040,000 km^2. It is surpassed only by the Amazonian tropical forests [1,2]. Recognized as a global biodiversity hotspot, the Cerrado is characterized by a humid tropical climate, with similar maximum monthly temperatures during both summer and winter. This ecosystem experiences a well-defined rainy season from October to May, and a dry season from June to September [3]. The native vegetation varies in composition, with increasing vegetation cover ranging from savanna grasslands (lacking trees) to woodland savannas [4,5]. Small scattered trees (open canopies) are typically observed in most woodland areas, where soil exposures and herbaceous vegetation on the ground are detectable by satellite sensors [6].

The rapid expansion of crops and cultivated pastures, driven by the adoption of soil and crop management practices in the Cerrado, has led to the clearing of approximately half of its native vegetation, according to the Action Plan for the Prevention and Control of Deforestation and Wildfires in the Cerrado Biome (PPCerrado). The Cerrado has therefore become one of the world's most important regions for grain production and livestock farming. Thus, in this fragmented landscape, the presence of various protected areas of savanna native vegetation provides a valuable opportunity to investigate vegetation phenology in response to seasonal and interannual patterns of precipitation.

In the Brazilian savanna, the phenology of native vegetation is heavily influenced by changes in precipitation, which affect the timing of seasonal cycles or phenophases [7–9]. Phenological changes in the Cerrado are therefore highly sensitive to climatic fluctuations across the different seasonal cycles. In addition to precipitation, disturbances such as fire, both natural and human-induced events, change the vegetation physiognomy and structure, influencing species abundance and diversity [10–13]. Projected climate change scenarios indicate a likely increase in fire frequency and a reduction in plant growth, driven by warmer and especially drier conditions [14]. In the Brazilian savannas, this is expected to result in shorter fire-free periods affecting the development of grasslands and woodlands. The problem is exacerbated by the use of fire as a management tool in agricultural practices, especially in the northern portion of the Cerrado biome, which serves as a major ignition source for wildfires spreading into surrounding native vegetation. The increasing human occupation and the modification in the natural fire regime have contributed to Cerrado accounting for approximately 70% of Brazil's burned areas [15].

Fire affects foliage cover and introduces variability in the phenological metrics of the different vegetation physiognomies. It has immediate effects on both vegetative and reproductive phenophases, affecting the number of flowers and fruits of woody species, and enhancing vegetative propagation of herbs and shrubs [16]. However, as reported by Silvério et al. [16], the long-term persistence of fire effects and their influence on the timing of vegetative phenological events in the savanna physiognomies of the Brazilian Cerrado remain unclear. Although these events are common throughout the biome and frequent during the local dry season (June to September), the impact of this disturbance on the determination of phenological metrics, such as Amplitude (AMP), Start (SOS), and End (EOS) of the growing season, and seasonal integrals, remains largely unexplored in the Brazilian savannas. Understanding how vegetation phenology varies in response to changes in precipitation, as well as the effects of fire and post-fire savanna regrowth in affected areas, is crucial for conservation planning and monitoring [17,18]. Thus, given that changes in environmental conditions can influence vegetation responses [19–21], this research is important for understanding phenological variations under climate change and, consequently, for supporting strategies to conserve the biome [22].

In savanna-protected areas in Brazil, studies of Land Surface Phenology (LSP), which derive vegetation phenological metrics from satellite observations, are the only viable option for conducting large-scale investigations. These studies can complement field phenological observations, which typically focus on individual species [23,24]. However, research analyzing the LSP of native vegetation from the Cerrado biome remains limited, hindering our understanding of the relationships between precipitation, fire, and various phenological metrics that describe vegetation dynamics across different seasonal cycles. From the set of available orbital instruments, the Moderate Resolution Imaging Spectroradiometer (MODIS) offers valuable opportunities for monitoring vegetation changes in shrubland and grassland ecosystems [25]. However, one reason for the scarcity of LSP studies using MODIS in the Cerrado is the small size of some protected areas, including ecological stations, parks, or conservation units. With a few exceptions, most of these preserved areas are inadequately viewed at the 250-m spatial resolution of MODIS. However, for large protected areas such as the EMAS National Park (ENP), observations from the MODIS MOD13Q1 product provide over 20 years of temporal coverage at 16-day composite intervals and 250-m spatial resolution [26]. In principle, this product enables long-term analysis of the NDVI response of Brazilian savannas to changes in precipitation across dry and wet seasonal cycles, as captured through long-term rainfall data from meteorological stations. Using software such as TIMESAT (version 3.3), a package to analyze time-series of satellite sensor data, several phenological metrics can be extracted, including the duration of the season, the changes in the vegetation index over the seasonal cycles, and the rates of vegetation greening and senescence [27–29].

To address the spatial resolution limitations of the MODIS instrument in monitoring small protected areas of the Cerrado, studies focused on vegetation classification have considered sensors with higher spatial resolution [30–32]. More recently, the Harmonized Landsat Sentinel (HLS) product, with a 30-m spatial resolution [33,34], has emerged as a promising alternative for examining LSP in response to precipitation and fire across various savanna physiognomies in the Cerrado biome—an application that remains unexplored. The HLS product offers harmonized time series data from Landsat and Sentinel satellites, with observation frequencies ranging from two to three days during the dry season of the Brazilian savannas (June to September). In the rainy season (October to May), the frequency of observations decreases with increasing cloud cover in Brazil. With its 30-m spatial resolution and high frequency of satellite observations during the dry season, when most wildfires occur, the HLS product also enhances environmental monitoring of such dynamic events. It enables the potential selection of control sites situated near burned areas within the same savanna vegetation type, which is essential to track vegetation recovery after fire disturbance.

At the ENP, the Park's Management Plan prioritizes research, monitoring, and fire control activities as essential strategies for conserving native vegetation. For example, firebreaks and controlled burns have been implemented over the past few decades to prevent the occurrence and spread of fires [35]. By reducing the accumulation of dry biomass (fire fuel), these management actions have lowered the likelihood of large wildfire events in the park. Despite these efforts, the ENP has experienced three major wildfire events between 2002 and 2023, which have affected significant portions of the park's area: 45% in 2005, 90% in 2010, and 21% in 2021. At the ENP, characterizing the seasonal behavior of LSP metrics, such as Amplitude (AMP), Base Level (BL), End of Season (EOS), Large Seasonal Integral (LSI), and Small Seasonal Integral (SSI), is essential, as these indicators reflect ecosystem conditions. Long-term trend analysis of these metrics is also crucial for understanding climate–vegetative interactions. However, before evaluating changes in their temporal trends, it is essential to develop a clearer understanding of the variability driven by fire, a key factor in vegetation phenology studies within savanna ecosystems. To address this gap in the literature on the Brazilian savannas, further research is needed to assess the relative influence of fire on the determination of LSP metrics, especially in comparison to the effects of precipitation.

In this study, we assessed for the first time the effects of both precipitation and fire on NDVI-derived phenological metrics at the ENP, a protected savanna area in central Brazil. These metrics were calculated using the TIMESAT software, along with the MODIS MOD13Q1 and HLS products, across grassland and woodland areas. More specifically, the study aims to: (i) identify the driest and wettest seasonal cycles at the ENP during the MODIS data analysis period (2002–2023), using a 40-year rainfall time series from a meteorological station to determine rainfall patterns; (ii) examine the relationships between precipitation and each of the 13 TIMESAT phenological metrics derived from the 250-m MODIS MOD13Q1 product in both grassland and woodland areas of the park; and (iii) investigate the influence of fire and vegetation recovery in burned areas on the determination of LSP metrics in pre- and post-disturbance seasonal cycles, using the 30-m spatial resolution HLS product, which combines data from the Landsat and Sentinel-2 satellites.

2. Methodology

The key methodological steps employed in the development of this work are summarized in Figure 1. Each step is detailed in the following subsections.

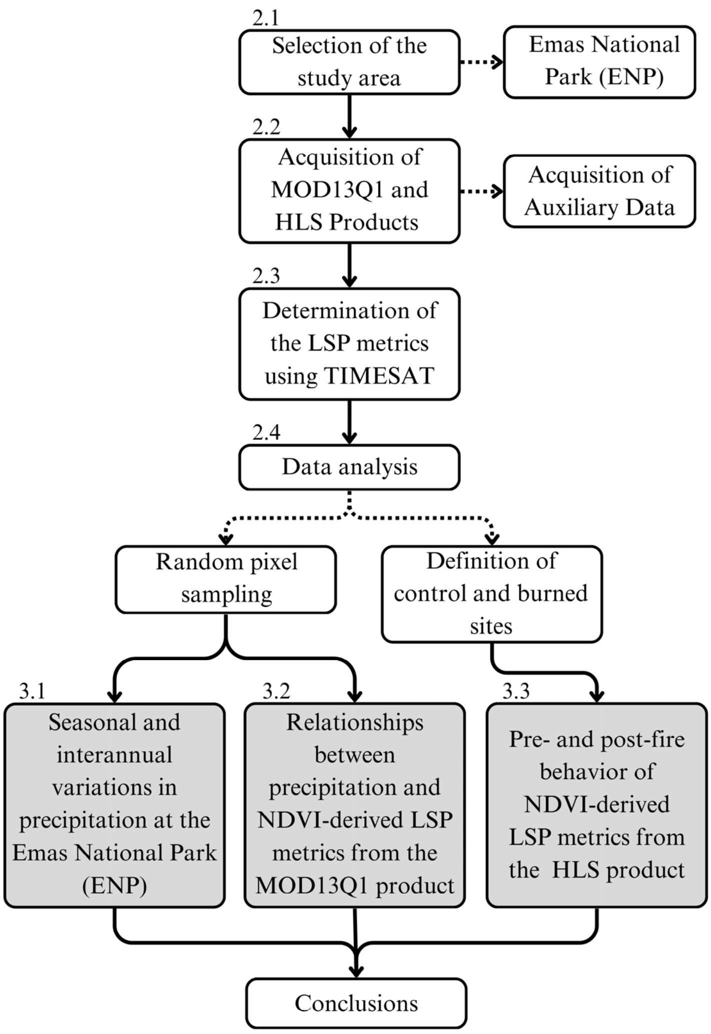

Figure 1. Summary of the key methodological steps employed in the study of the effects of precipitation and fire on NDVI-derived phenological metrics in Brazilian savannas. The numbered boxes are described below in the subsections.

2.1. Selection of the Study Area

Created in 1961 and located in the state of Goiás, in central Brazil, the ENP was chosen as the study area for three primary reasons (Figure 2). First, this protected area (a Conservation Unit) encompasses vegetation physiognomies that are representative of the Cerrado biome, including savanna grasslands and shrub savannas (referred here to as "grasslands") as well as wooded savannas and woodland savanna (referred to as "woodlands"). Second, the ENP is the largest protected park within this biome, covering an area of 1328 km^2, which facilitates observations using MODIS (250-m MOD13Q1 product) and Landsat/Sentinel-2 (30-m HLS product) data. Third, three large fire events were recorded during the study period (2002–2023), as detailed later, making the park an ideal site for our experimental design.

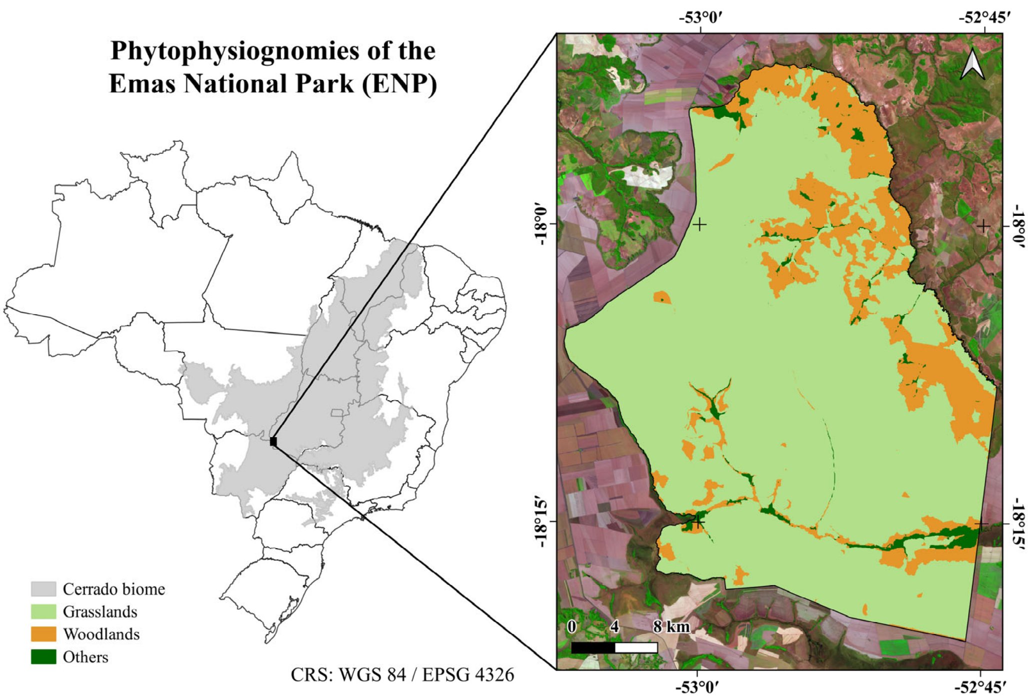

Figure 2. Location of the Emas National Park (ENP) in the state of Goiás, central Brazil. The vegetation map highlights the predominant occurrence of grasslands (savanna grassland and shrub savanna physiognomies) and woodlands (wooded savanna and woodland savanna physiognomies). Areas classified as 'Others' include riparian forests and small patches of seasonal semideciduous forests. The vegetation map was adapted from Batista [36].

Fire management is a common practice at ENP. Controlled burns and firebreaks (wide, vegetation-free corridors) are integral components of this strategy. When combined, these actions prevent the accumulation of dry biomass on the ground (fire fuel), creating also barriers that inhibit the spread of fire [35]. These practices have reduced both the frequency and impact of human-induced fires, which usually start in the vicinities of the park. Large fire events, affecting significant portions of the park, previously occurred every three years, having decreased in frequency in more recent decades.

The ENP has well-defined rainy (October to May) and dry (June to September) seasons, with an average annual precipitation of 1600 mm. The mean annual temperature is 23 °C [36]. Most of the ENP is located at the top of a plateau with gentle terrain and altitudes ranging from 800 to 900 m, especially in grassland areas (Figure 2). At the northeast of the park (woodland areas), the relief is more undulated. The predominant soil types, according to the Brazilian System of Soil Classification, include *Latossolo Vermelho-Escuro dis-*

trófico and *Latossolo Vermelho-Amarelo distrófico* [35,37], or red and yellowish-red Dystrophic Ferralsol, respectively.

2.2. Acquisition of MOD13Q1 and HLS Products and Auxiliary Data

Two satellite products were used to retrieve LSP metrics from the NDVI data: the MOD13Q1 product (version 6.1) and the HLS product (version 2.0). The MODIS MOD13Q1 product provides NDVI composite images at 16-day intervals with a spatial resolution of 250 m. The final NDVI value for each pixel represents the highest record within the 16-day observation period. This approach allows the algorithm to discard noisy pixels affected by clouds, residual atmospheric contamination, and large view zenith angles or off-nadir viewing [26].

The Harmonized Landsat Sentinel-2 (HLS) product provides a series of surface reflectance images from the Operational Land Imager (OLI), on the Landsat 8 and 9 satellites, and the Multi-Spectral Instrument (MSI), on the Sentinel 2A and 2B satellites. The pre-processing and harmonization steps include atmospheric correction; cloud and cloud-shadow masking; spatial co-registration and common gridding; illumination and view angle normalization; and spectral bandpass adjustment [33]. As a result, the product has a temporal resolution ranging from 2 to 3 days and a spatial resolution of 30 m. The HLS product offers individual spectral bands, and thus, the Red and Near Infrared (NIR) bands necessary to calculate the NDVI [34].

Ancillary data included two main types of observations: a vegetation map published by Batista [36] and rainfall data from the nearest meteorological station to the park, located in the municipality of Chapadão do Céu (GO). The major vegetation physiognomies mapped by Batista [36] were grouped in our study into three classes: (i) grasslands, comprising savanna grasslands and shrub savannas; (ii) woodlands, including wooded savannas and woodland savannas; and (iii) others, consisting of riparian forests and small patches of seasonal semideciduous forests. We focused our analysis on the two broad savanna classes: grasslands and woodlands.

The meteorological station used in our study has provided data since 1983, enabling a precise analysis of the local rainfall regime based on average values calculated over a period of at least four decades, as defined by a Climatological Normal. The daily rainfall records are collected by the National Hydrometeorological Network (RHN) and made available through the HidroWeb Portal, which is part of the National System of Water Resources Information (SNIRH). The data spreadsheet includes four possible collection statuses: 0 = Blank; 1 = Real; 2 = Estimated; 3 = Doubtful; and 4 = Accumulated. The data were carefully reviewed, and those marked as “doubtful” were replaced with the average rainfall for the same day from other years in the series. The “accumulated” values were retained, as they represent the sum of rainfall (in mm) over a sequence of days. In our study, we calculated both the accumulated rainfall for the rainy season of each growing cycle between 2002 and 2023, covering October to May, and the total accumulated annual rainfall per cycle, spanning from October to September.

2.3. Determination of the LSP Metrics Using TIMESAT

LSP metrics were derived from NDVI data obtained from both the MODIS MOD13Q1 and HLS products using the TIMESAT software. A summarized description of the 13 LSP metrics is presented in Table 1. The NDVI, introduced by Rouse et al. [38], is one of the most widely used vegetation indices in remote sensing studies. By utilizing the normalized difference between the reflectance of the NIR and Red bands, NDVI is sensitive to vegetation structure and leaf pigments. Compared to other indices, such as the Enhanced Vegetation Index (EVI), which is also available in the MOD13Q1 product, NDVI is generally less affected by factors like viewing-illumination geometry and canopy-terrain shadows [39–41]. Additionally, NDVI does not saturate under the sparse vegetation conditions typical of Brazilian savannas.

Table 1. Land Surface Phenology (LSP) metrics calculated from TIMESAT based on NDVI. The description of each metric was adapted from Eklundh and Jönsson [27].

LSP Metric	Abb.	Description	Unit
Start of Season	SOS	Start time of growing season	DOY
End of season	EOS	End time of growing season	DOY
Length of the Season	LOS	Duration of the season	Days
Time for the Mid of the Season	TMS	Mean value of the times for which, respectively, the left edge has increased to the 80% level and the right edge has decreased to the 80% level	DOY
Largest Data Value	LDV	Largest NDVI in the season	-
Base Level	BL	Average of the left and right minimum NDVI values	-
Amplitude	AMP	Difference between LDV and BL	-
Value for the Start of the Season	VSS	NDVI value of the function at the time of SOS	-
Value for the End of the Season	VES	NDVI value of the function at the time of EOS	-
Rate of Increase at the Beginning of the Season	RIBS	Ratio of the difference between the left 20% and 80% levels and the corresponding time difference	NDVI/DOY
Rate of Decrease at the End of the Season	RDES	Ratio of the difference between the right 20% and 80% levels and the corresponding time difference	NDVI/DOY
Large Seasonal Integral	LSI	Integral of the function describing the season from the SOS to the EOS	NDVIxDOY
Small Seasonal Integral	SSI	Integral of the difference between the function describing the season and the BL	NDVIxDOY

TIMESAT is one of the most widely used software for retrieving LSP metrics in vegetation phenology studies. Originally designed to handle time series of NDVI data, it now supports other datasets as well [27,42]. In our study, TIMESAT (version 3.3) was applied to the regularly spaced time series of MODIS NDVI data (16-day spaced intervals) and to the irregularly spaced time series of HLS data, which were converted into regular intervals of 5 days through interpolation and gap filling. In order to ensure data quality, we used the ancillary pixel reliability information from the MOD13Q1 product. We assigned weights of 1.0, 0.5, and 0.0 to pixels classified as good (code 0), marginal (code 1), and cloudy (code 3), respectively. In our study area, good-quality pixels (code 0) generally increased from the rainy season (October to May) to the dry season (June to September), as shown for 2019 in Figure A1 (Appendix A). Cloud-free pixels were considered also in the HLS product. After defining the number of seasons and their approximate timing, a smoothing function was applied to the data using the Savitsky-Golay filter. This filter has been used in many studies of vegetation phenology e.g., [43–46]. Furthermore, this filter was more efficient in reducing noise than the other options available in TIMESAT.

After smoothing the NDVI time series from both the MODIS MOD13Q1 and HLS products, the following 13 LSP metrics were extracted (Table 1): Start of the Season (SOS), End of the Season (EOS), and Length of the Season (LOS); Time for the Mid of the Season (TMS); Largest Data Value (LDV); Base Level (BL); Amplitude (AMP); NDVI Value at the Start (VSS) and End (VES) of the Season; Rate of Increase at the Beginning of the Season (RIBS); Rate of Decrease at the End of the Season (RDES); and the Large Seasonal Integral (LSI) and Small Seasonal Integral (SSI). A graphical representation of most of these metrics is shown in Figure 3. Details can be found in several references e.g., [27,47].

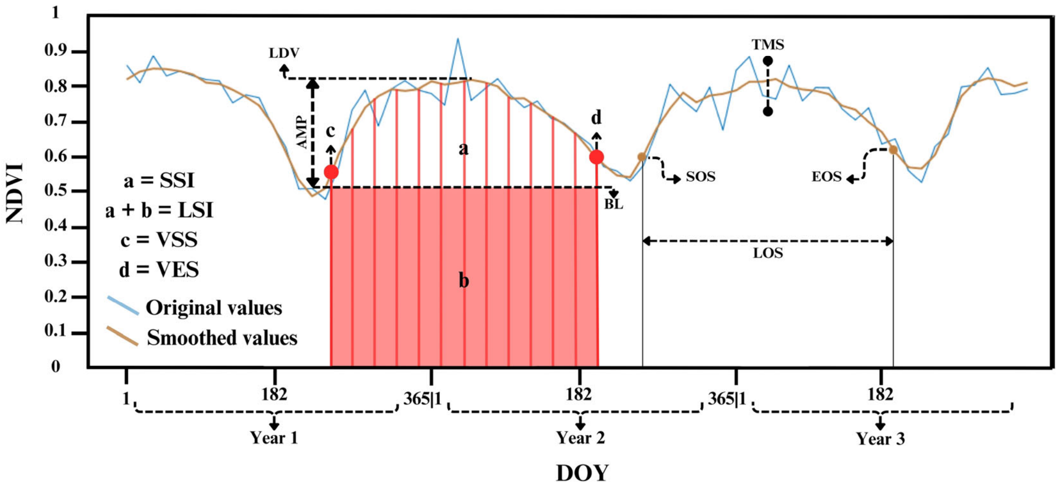

Figure 3. Example of the seasonal NDVI variations in woodland savanna from the Emas National Park (ENP) with a graphical representation of the TIMESAT metrics used in the data analysis. The abbreviations are: SOS (Start of Season), EOS (End of Season), TMS (Time for the Mid of the Season), AMP (Amplitude), BL (Base Level), LDV (Largest Data Value for the fitted function during the season), VES (Value for the End of the season), VSS (Value for the Start of the season), LOS (Length of Season), LSI (Large Seasonal Integral), and SSI (Small Seasonal Integral). The Rate of Increase at the Beginning of the Season (RIBS) and the Rate of Decrease at the End of the Season (RDES) were omitted for better graphic representation.

2.4. Data Analysis

The data analysis was divided into three linked steps: (i) identifying the driest and wettest growing season cycles at the ENP during the period of analysis (2002–2023); (ii) investigating the correlations between accumulated precipitation during each of the 21 growing season cycles and the corresponding MODIS LSP metrics; and (iii) exploring the impact of fire and vegetation recovery in burned areas on the determination of both the MODIS and HLS LSP metrics.

The first part of the analysis, which supported the subsequent examination of the relationships between rainfall and LSP metrics, used rainfall data from the meteorological station (1983–2023) near the ENP. To identify dry and wet growing season cycles, the boxplot approach was adopted. Following the procedures outlined by Galvani and Luchiari [48], we used a box plot to categorize the park's rainfall regime into five distinct categories: severely dry, dry, regular, wet, and severely wet. In interpreting the boxplot, each quartile represents 25% of the data in the time series and corresponds to a specific category. Values that exceed the thresholds (upper and lower fences) indicate cycles classified as severely wet or severely dry, respectively. The hydrological cycle was defined as ranging from October of a given year to September of the following year, thus covering a full seasonal cycle. Consequently, the total rainfall for each seasonal cycle from 1983 to 2023 was used to generate the boxplot and to define the dry and wet cycles for the ENP during the MODIS data analysis from

2002/2003 to 2022/2023. This approach provided a comprehensive analysis of rainfall patterns across the seasonal cycles, accounting for the Climatological Normal.

In the second step of the data analysis, we correlated the accumulated rainfall during the rainy season (October to May) across each of the 21 seasonal cycles (2002/2003 to 2022/2023) with the corresponding average values of the 13 MODIS TIMESAT metrics calculated for grassland and woodland areas (Table 1). To obtain the MODIS LSP means and calculate Pearson's correlation coefficients (r values), we applied a random computational sampling of 500 pixels per vegetation class (grassland and woodland). Our analysis focused specifically on the rainy season of each growing season cycle, which typically accounts for approximately 95% of the total precipitation from the cycle at the ENP. To complement the correlation analysis and minimize the impact of fire and burned areas on the results, the LSP metrics most strongly correlated with precipitation were selected and their relative frequency histograms were plotted for the driest and wettest cycles, excluding those affected by large fire events at the ENP. Then, we evaluated statistical differences between the two population means (driest and wettest) for each LSP metric at the 0.05 confidence level.

In the final step of the data analysis, we investigated the effects of fire and resultant vegetation recovery in burned areas on phenological metrics derived from the MODIS MOD13Q1 and HLS products. During the period of analysis (2002 to 2023), the ENP was affected by three major human-induced fires: one that began on 1 September 2005, impacting 45% of the park's area; another that started on 12 August 2010 (90% of the park's area); and a third event that ignited on 10 July 2021 (21% of the park's area). Thus, all fire events occurred during the local dry season. In the data analysis, the spectral profiles of the MODIS NDVI and its derived TIMESAT metrics were examined for these three events, using the same set of randomly selected pixels from the previous rainfall analysis (500 pixels for grasslands and 500 pixels for woodlands).

Due to the inherent bias in pixel sampling for burned areas, which ranged in extent from 21% (2021 event) to 90% (2010 event), and the challenges in selecting control sites within the 250-m MODIS MOD13Q1 product, our experimental design was redefined. We then focused on the 2021 fire event and on the LSP metrics derived from the reprocessed 5-day, 30-m harmonized HLS product. The 2021 event was the only one of the three fire events covered by this product. Using satellite images from the HLS product, we selected a control site (non-burned area) located near a burned site. Both the control and burned sites (size of 2 km $\times$ 2 km each) are therefore composed of the same vegetation type (grasslands) and have experienced the same amount of precipitation during a given pre- or post-fire seasonal cycle.

For each site (control and burned), with location further indicated in Results (color composites), we randomly sampled 500 pixels without replacement. For each LSP metric, we compared the difference between control and burned sites in the seasonal cycle preceding the fire (2019/2020), during the fire event (2020/2021), and in the post-fire cycles (2021/2022 and 2022/2023). In addition to using *p*-values to detect statistically significant differences between the means of two populations (control and burned sites), we calculated the magnitude of the impact caused by fire and burned areas on the determination of vegetation phenological metrics. We measured the standard deviation of the difference through the calculation of Hedge's G metric [49]. The Hedge's G was calculated for each of the 13 HLS-derived LSP metrics for the control and burned site pairs of data across these mentioned seasonal cycles (2019/2020 to 2022/2023). The analysis of the LSP differences between sites in the pre-fire cycle served as an indirect measure of uncertainties in LSP determination using the HLS product. In contrast, the post-fire cycle analysis allowed for the evaluation of vegetation recovery in the burned areas. Additionally, relative frequency histograms of the HLS-derived TIMESAT metrics, along with corresponding images, were generated and plotted to consolidate the analysis and interpretation of results.

3. Results

3.1. Identification of the Driest and Wettest Seasonal Cycles at the Park

The analysis of long-term average monthly precipitation (1983–2023) at the ENP confirmed the occurrence of a rainy season from October to May and a dry season from June to September (Figure 4). During the dry season, monthly rainfall typically falls below 50 mm. In the more recent years, between 2018 and 2021, no rainfall exceeding 6 mm was recorded for June, July, and August, indicating a notably local dry winter. However, as shown by the outliers in Figure 4, there were a few years, especially between 2014 and 2017, when the accumulated rainfall in these months unusually exceeded 100 mm with the majority of precipitation occurring in June.

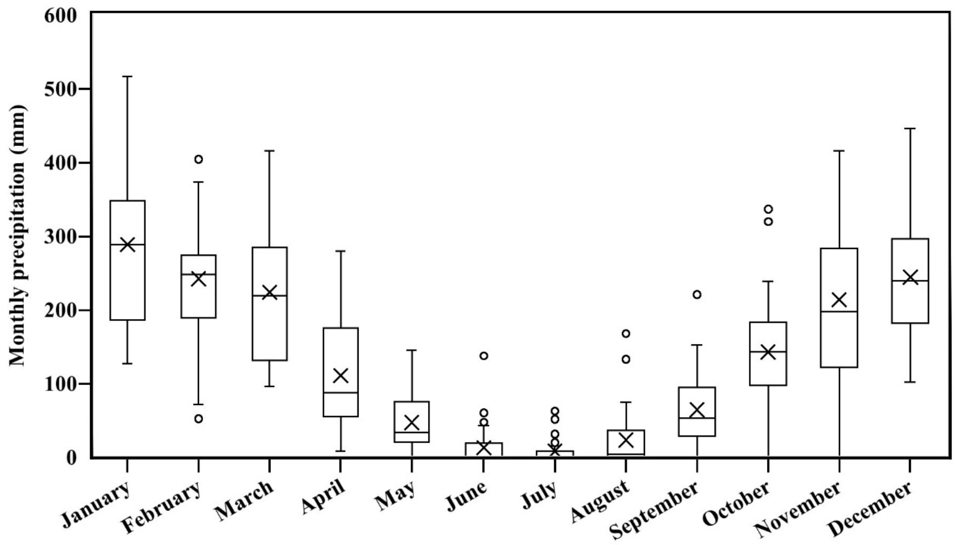

Figure 4. Variations in average long-term monthly precipitation (1983–2023) at Emas National Park (ENP). The mean values are represented by crosses, while the median values are shown as horizontal lines within the boxes for each month. Outliers are depicted as circles.

Interannual variations in accumulated precipitation on each cycle during the period of MODIS data analysis (2002/2003 to 2022/2023 cycles), compared to the long-term 1983–2023 period, are shown in the boxplot of Figure A2 (Appendix A). The results from the boxplot analysis of long-term rainfall data (1983–2023) from the meteorological station identified the following intervals of accumulated precipitation per cycle: severe dry cycle (<1153 mm), dry (1153–1433 mm), regular (1433–1814 mm), wet (1814–2057 mm), and severe wet cycle (>2057 mm). However, as shown in Figure 5, no severe dry or wet cycles were detected during the period of MODIS data analysis. The seven dry cycles that deviated from the Climatological Normal were 2002/2003, 2004/2005, 2005/2006, 2006/2007, 2020/2021, 2021/2022, and 2022/2023, as indicated by the red color in Figure 5. The eight wet cycles detected in our analysis were 2009/2010, 2010/2011, 2011/2012, 2013/2014, 2014/2015, 2015/2016, 2018/2019, and 2019/2020 (blue color in Figure 5). The remaining six cycles were classified as regular cycles in the boxplot analysis when compared to the 1983–2023 long-term rainfall (gray color in Figure 5).

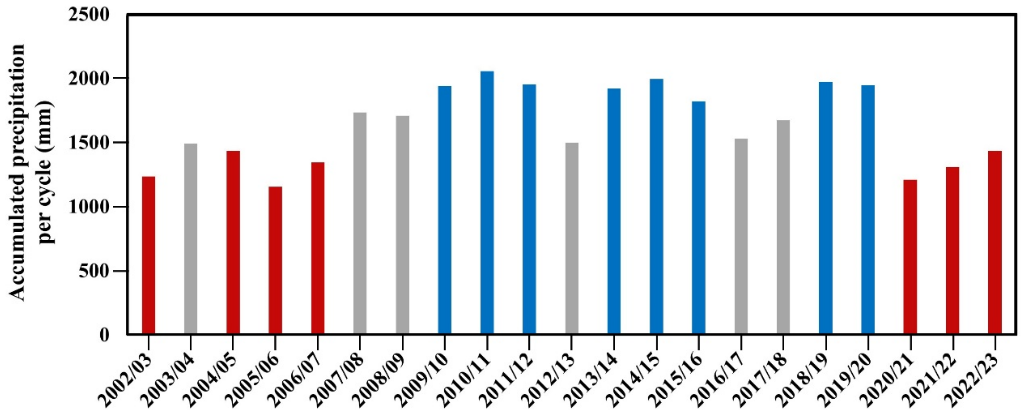

Figure 5. Accumulated precipitation during the rainy season of each studied seasonal cycle, highlighting the occurrence of wet (blue), regular (gray), and dry (red) growing season cycles at Emas National Park (ENP). Rainfall patterns were identified through a boxplot analysis of long-term precipitation data (1983–2023) collected by a local meteorological station. Severely dry or wet cycles were not detected in the MODIS period of analysis (2002/2003 to 2022/2023).

3.2. Relationships Between Precipitation and NDVI-Derived LSP Metrics from the MOD13Q1 Product

Variations in MODIS NDVI throughout the 2007/2008 seasonal cycle (October 2007 to September 2008) are presented in Figure 6 for grassland and woodland areas (n = 500 pixels per vegetation class). These variations are representative of the patterns observed in the other cycles. The transition from grasslands to woodlands was characterized by increasing NDVI values with increasing vegetation cover, along with a smaller difference between the minimum and maximum NDVI observed during the dry and rainy seasons, respectively. For both vegetation types, the NDVI curves generally reproduced the seasonal rainfall pattern. The 2007/2008 growing season began with the onset of the rainy season from September to October 2007, leading to a rise in NDVI values in tandem with rainfall until May 2008. From June to the middle of September 2008, the NDVI declined as the water deficit increased during the dry season (Figure 6). In the 2007/2008 cycle, the highest NDVI values were observed in January (around DOY 017), while the lowest values occurred in September (around DOY 250) at maximum water deficit.

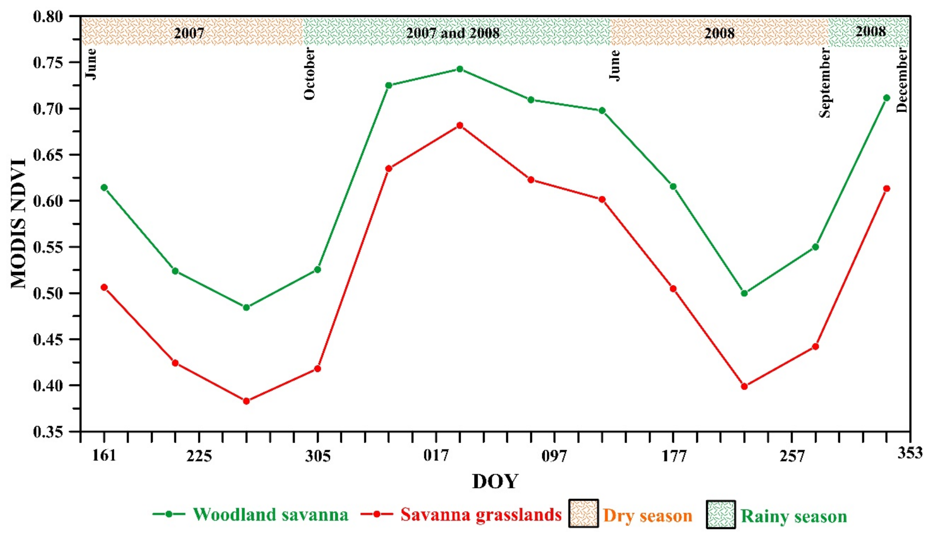

Figure 6. Average MODIS NDVI variations in areas of woodlands and grasslands at the EMAS National Park (ENP) during the 2007/2008 seasonal cycle (October 2007 to September 2008). The local dry and rainy seasons are indicated at the top of figure.

The mean and standard deviation values, calculated from the 21 seasonal cycles (2002/2003 to 2022/2023), revealed substantial variability in most of the MODIS NDVI-derived LSP metrics (Table 2). Compared to grasslands, woodland areas exhibited lower mean values of SOS and higher mean values of EOS, resulting in a slightly longer growing season, as indicated by LOS. However, the observed nine-day difference in LOS was smaller than the 16-day interval used to generate the MODIS MOD13Q1 composite product. The mean values of BL, LDV, LSI, TMS, VES, and VSS generally increased with vegetation cover towards the woodlands, while average AMP and SSI followed an opposite trend. No significant differences in RDES and RIBS were observed between the two broad classes of vegetation.

Table 2. Variations in MODIS NDVI-derived Land Surface Phenology (LSP) metrics across seasonal cycles from 2002/2003 to 2022/2023 for grassland and woodland areas.

LSP Metric	Grasslands	Woodlands
AMP	0.311 ± 0.061	0.290 ± 0.054
BL	0.388 ± 0.054	0.480 ± 0.057
EOS (DOY)	199.732 ± 22.937	206.030 ± 20.739
LDV	0.698 ± 0.051	0.772 ± 0.047
LOS (DOY)	300.038 ± 47.277	309.097 ± 45.753
LSI	11.838 ± 1.313	13.767 ± 1.366
RDES	0.036 ± 0.017	0.035 ± 0.013
RIBS	0.059 ± 0.029	0.057 ± 0.028
SOS (DOY)	264.693 ± 37.770	261.932 ± 38.435
SSI	3.959 ± 0.849	3.756 ± 0.759
TMS (DOY)	55.766 ± 59.080	58.971 ± 57.284
VES	0.450 ± 0.061	0.541 ± 0.056
VSS	0.446 ± 0.058	0.538 ± 0.055

After correlating the measured accumulated precipitation during the rainy season of each cycle with the corresponding MODIS LSP metrics, we found the highest positive correlations with metrics such as LSI, SSI, RIBS, EOS, and AMP, particularly over woodland areas (Figure 7). They were statistically significant at the 0.05 level. Examples of the relationships between rainy season cumulative precipitation and LSI in grassland areas, as well as SSI in woodland areas, are shown in Figures 8a and 8b, respectively. Both metrics exhibited a linear increase with rising precipitation across cycles, with Pearson's correlation coefficients of +0.575 for LSI in grasslands (Figure 8a) and +0.585 for SSI in woodlands (Figure 8b). In comparison to dry cycles, wet cycles prolonged the growing season, increased the amplitude of NDVI values relative to the baseline, and resulted in changes in the areas beneath the growing season NDVI curves.

After selecting two opposite cycles from Figure 5 (the dry 2006/2007 and the wet 2019/2020), unaffected by any of the three large fire events (2005, 2010, and 2021), we observed significant statistical differences in the LSP metrics highly correlated with precipitation. Supporting the correlation results from Figures 7 and 8, the LSI in grassland areas showed a t-value of -28.023 between these two cycles (Figure 9a), while the SSI in woodland areas had a t-value of -54.268 (Figure 9b), both with p-values less than 0.001. The negative t-values in Figure 9 indicate that the LSI, SSI, and other LSP metrics positively correlated with precipitation in Figure 7 were lower during the dry cycle compared to the wet cycle, confirming their increase with rainfall.

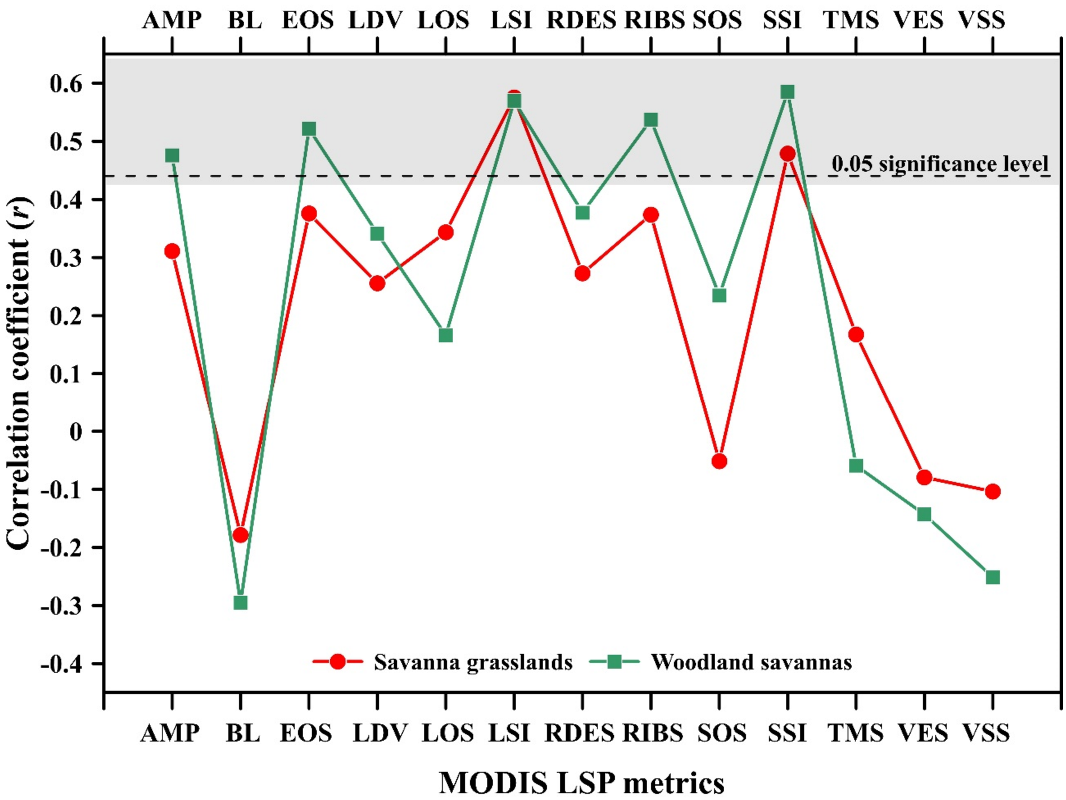

Figure 7. Pearson's correlation coefficients for the relationships between rainy season cumulative precipitation (total rainfall from October to May) of each seasonal cycle (2002/2003 to 2022/2023) and MODIS NDVI-derived LSP metrics. Results are presented for average values of selected pixels (n = 500 per seasonal cycle) representing grassland (red) and woodland (green) physiognomies. The horizontal dashed line denotes statistically significant relationships at the 0.05 level.

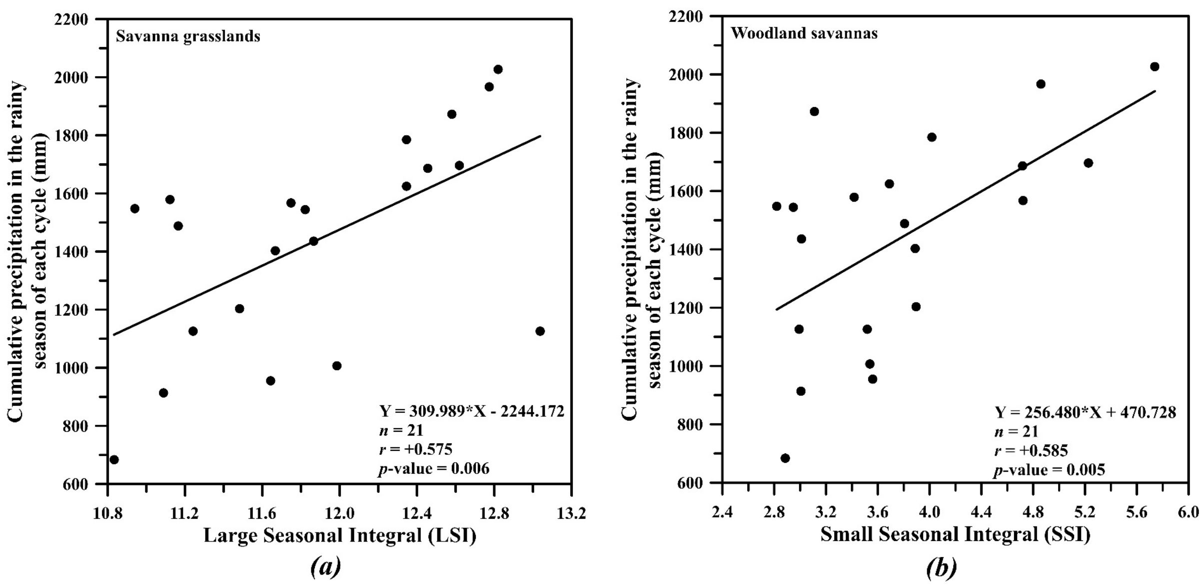

Figure 8. Relationships of the cumulative precipitation in the rainy season of each seasonal cycle (2002–2003 to 2022/2023) with the MODIS extracted metrics (**a**) Large Seasonal Integral (LSI) and (**b**) Small Seasonal Integral (SSI) in areas of grasslands and woodlands, respectively.

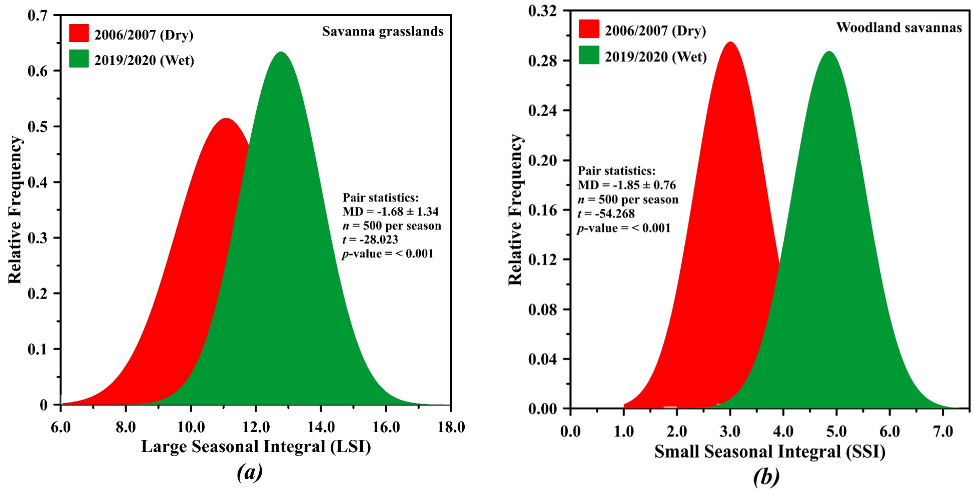

Figure 9. Pairs of Gaussian-fitted histograms showing statistical differences in MODIS NDVI extracted (**a**) Large Seasonal Integral (LSI) and (**b**) Small Seasonal Integral (SSI). Results are presented for the seasonal cycles of 2006/2007 (dry) and 2019/2020 (wet) over grassland and woodland areas, respectively. MD is the mean difference between the histograms.

3.3. Pre- and Post-Fire Behavior of NDVI-Derived LSP Metrics from the MOD13Q1 and HLS Products

From our results, the three largest fire events that occurred at ENP during the MODIS analysis period (2002–2023) affected the park's area and vegetation physiognomies in distinct ways. The first fire event began on 1 September 2005, lasting for five days, and impacted 45% of the park's area, including both grassland and woodland physiognomies. The second event, on 12 August 2010, lasted several days and affected all vegetation types, burning nearly the entire park (90% of its area). The third fire, which ignited on 10 July 2021, impacted only grasslands, burning 21% of the park's area over the course of three days.

These three events were tracked using false-color Landsat composites (Figure 10), highlighting pre-fire scenes (first column) and post-fire scenes (subsequent columns). Recently burned areas during the local dry season (second column) at ENP are shown in dark blue, while vegetation regeneration areas in the following rainy season (images from April and May) are depicted in red. Visual inspection of these color composites revealed burn scars clearly visible in the dry-season images of the cycles following the fire events (last column images in Figure 10). Thus, the effects of fire events in a given seasonal cycle were generally observed in satellite color composites of the subsequent seasonal cycle.

Using the same set of pixels from the previous rainfall analysis (500 per vegetation type) results from examining temporal profiles of various phenological metrics captured the impact of fire and burned areas on the determination of MODIS NDVI-derived phenological metrics (Figures 11 and 12). This examination across burned and non-burned seasonal cycles was obviously influenced by our sampling strategy, which covered the entire ENP area rather than focusing solely on the fire-affected zones. As a result, the effects of the 2005 (45% of the park's area) and 2021 (21%) fire events on LSP metrics were somewhat obscured in magnitude, when compared to the 2010 event, which burned almost the entire park. Focusing specifically on the 2010 event (marked by the orange vertical bar in Figure 11), we observed a decrease in some LSP metrics, such as BL (Figure 11a) and VES (Figure 11b). Consistent with the results in Table 2, both BL and VES increased with vegetation cover toward the woodland areas (Figure 11). In the case of BL, the fire effects were not only present in the seasonal cycle during which the event occurred (2009/2010 cycle) but also carried over into the subsequent cycle (2010/2011). In contrast, other LSP metrics, such as AMP (Figure 12a) and SSI (Figure 12b), showed an increase due to biomass burning and vegetation recovery in both seasonal cycles.

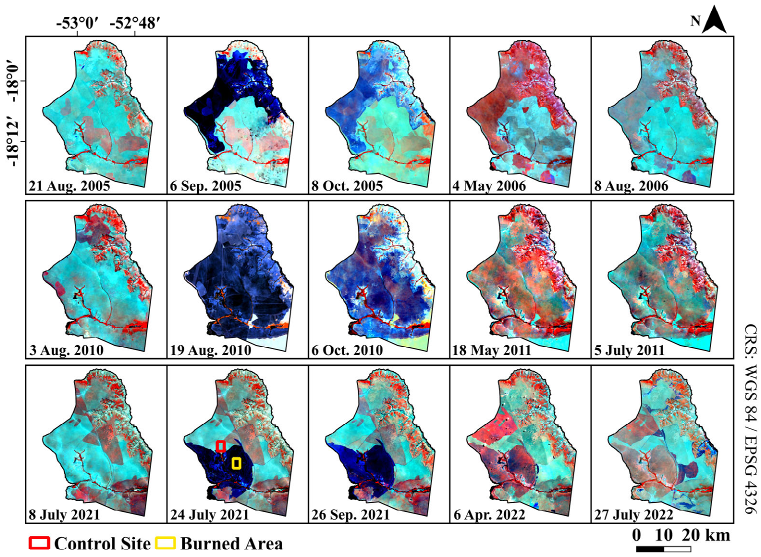

Figure 10. False-color composites of the Emas National Park (ENP) using the NIR, SWIR-1, and SWIR-2 Landsat bands in RGB, respectively. Images from TM/Landsat-5 (**top**), ETM+/Landsat-7 (**middle**), and OLI/Landsat-8 (**bottom**) depict the landscape before and after fire events on 1 September 2005 (affecting 45% of the park's area), 12 August 2010 (90%), and 10 July 2021 (21%), respectively. At the bottom, the locations of the selected control (non-burned) and burned sites are shown on the image from 24 July 2021. Burned areas are shown in dark blue, while vegetation recovery in these areas is depicted in red.

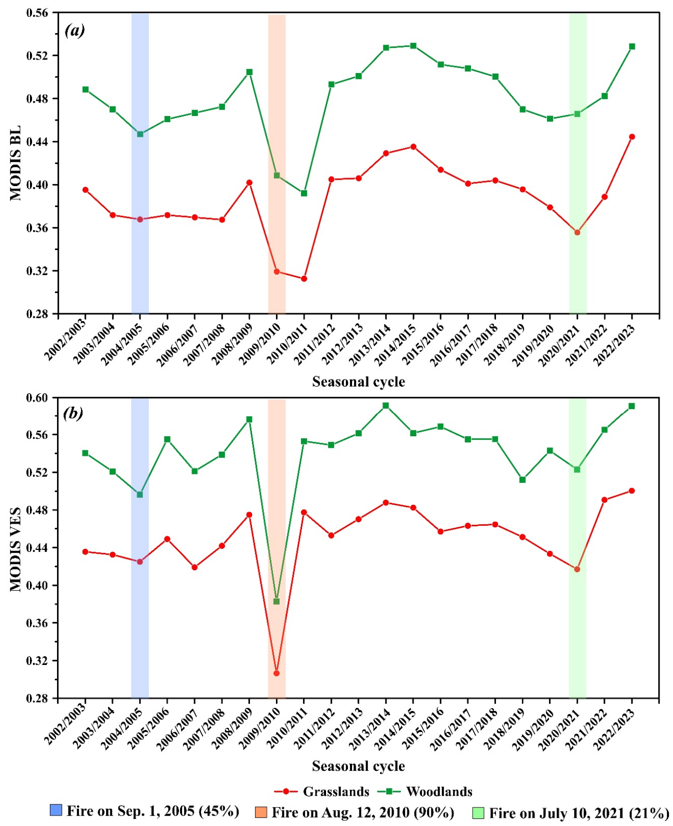

Figure 11. Interannual variations in the MODIS Land Surface Phenology (LSP) metrics (**a**) Base Level (BL) and (**b**) Value for the End of the Season (VES) in savanna grassland (red line) and woodland (green lines) areas from the EMAS National Park (ENP). Three major fire events during this period are highlighted by colored shaded columns: 1 September 2005 (affecting 45% of the park's area), 12 August 2010 (90%), and 10 July 2021 (21%).

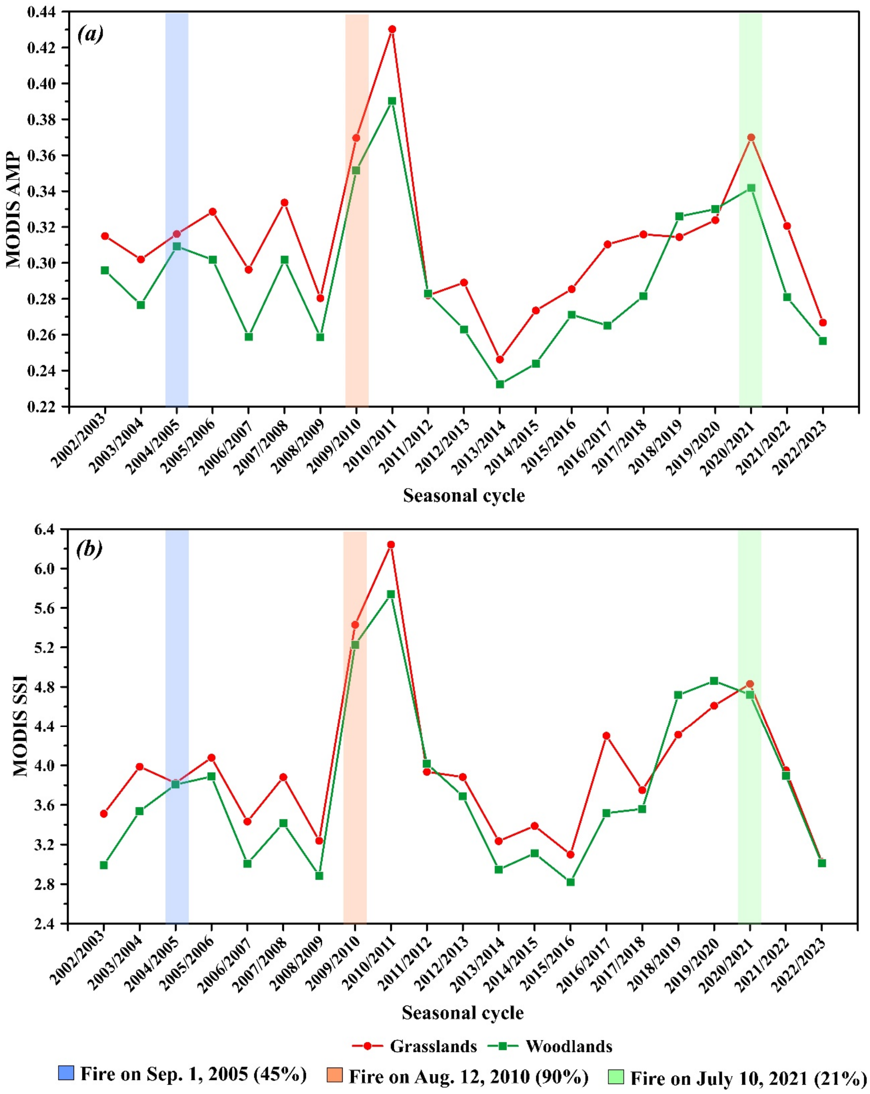

Figure 12. Interannual variations in the MODIS Land Surface Phenology (LSP) metrics (**a**) Amplitude (AMP) and (**b**) Small Seasonal Integral (SSI) in savanna grassland (red line) and woodland (green lines) areas from the EMAS National Park (ENP). Three major fire events during this period are highlighted by colored shaded columns: 1 September 2005 (affecting 45% of the park's area), 12 August 2010 (90%), and 10 July 2021 (21%).

A detailed analysis of the 2021 fire impact on the TIMESAT determination of phenological metrics, using the reprocessed 5-day 30-m harmonized HLS product, revealed the NDVI temporal patterns with grassland burning and subsequent vegetation recovery (Figure 13). By comparing a burned site with a neighboring control (non-burned) site in savanna grasslands (site location indicated in Figure 10), we observed a substantial decrease in NDVI, dropping from approximately 0.40 to 0.10 on 10 July 2021, when the fire began during the local dry season of the 2020/2021 cycle (dashed circle in Figure 13). After the start of the rainy season in October 2021, marking the beginning of the following seasonal cycle (2021/2022), vegetation starts to recover strongly, leading to an increase in NDVI towards December, when similar NDVI values were observed between the control and burned sites (dashed square in Figure 13). From December until the end of the following 2021/2022 dry season in September 2022, the recovery of grasses led to higher NDVI values in the burned areas compared to the control site. Comparable NDVI values between the control and burned sites were observed in October 2022 with the beginning of the new 2022/2023 seasonal cycle (Figure 13). Therefore, the impact of burned areas on the decrease in NDVI was observed during the 2020/2021 cycle (disturbance cycle), while vegetation recovery effects became evident in the following seasonal cycle (2021/2022). These effects were minimal during the 2022/2023 cycle. Compared to grasslands of the burned site, the structural and floristic composition of some burned woody species may take more years to recover, as will be discussed later.

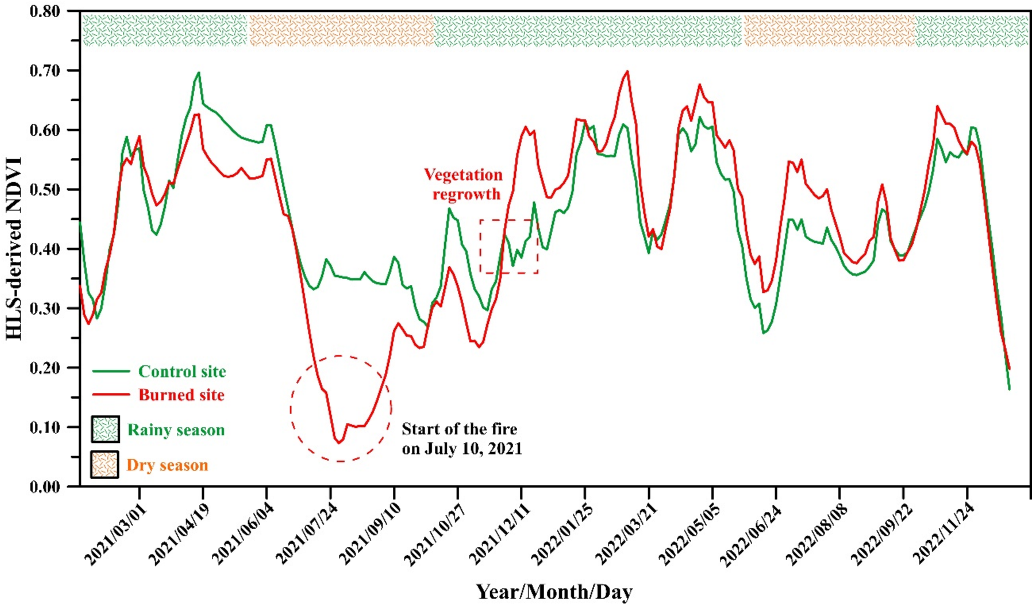

Figure 13. Seasonal variations in HLS-derived NDVI, highlighting the effects of 2021 fire event and resultant burned area on NDVI response of savanna grasslands. In comparison with the control site, this event is marked by a decrease in the NDVI (dashed circle in red) during the dry season (symbols in orange at the top of figure) of the 2020/2021 cycle, and by a notable post-burning vegetation recovery at the start of the subsequent rainy season (symbols in green at the top of figure) from the following 2021/2022 cycle. The dashed square indicates the intersection point of the NDVI response for burned and non-burned grassland sites.

The analysis of the fire's effect size on the HLS-derived NDVI phenological metrics confirmed the MODIS results from Figures 11 and 12. To illustrate this, we plotted the Hedge's effect size metric (Figure 14). The results showed the statistical differences for each LSP metric between control and burned sites, considering the seasonal cycles before the fire (2019/2020), during the fire event (2020/2021), and after the fire (2021/2022 and 2022/2023 cycles). Positive values of Hedge's G indicated that the values of the control site were higher than those of the area affected by the fire. When considering the Hedge's G values outside the limits defined by the shaded horizontal bar in Figure 14, which represents an indirect measurement of uncertainties in the control site, the most affected phenological metrics were BL, VES, and VSS, which decreased in burned areas during both the 2020/2021 and 2021/2022 seasonal cycles. The effects on VSS were notably stronger in the seasonal cycle following the fire event, as indicated by the relative behavior of the red (2020/2021 cycle) and magenta (2022/2023 cycle) lines in Figure 14 for this metric. In contrast, metrics such as AMP and SSI increased as a result of the fire impact in these two cycles (Figure 14). The effect size analysis also identified EOS as a sensitive metric to fire-affected areas. However, upon reviewing Figure A3 in Appendix A, we observed that the average EOS showed only small differences (approximately 10 days) between control and burned sites for both the pre- and post-fire seasonal cycles.

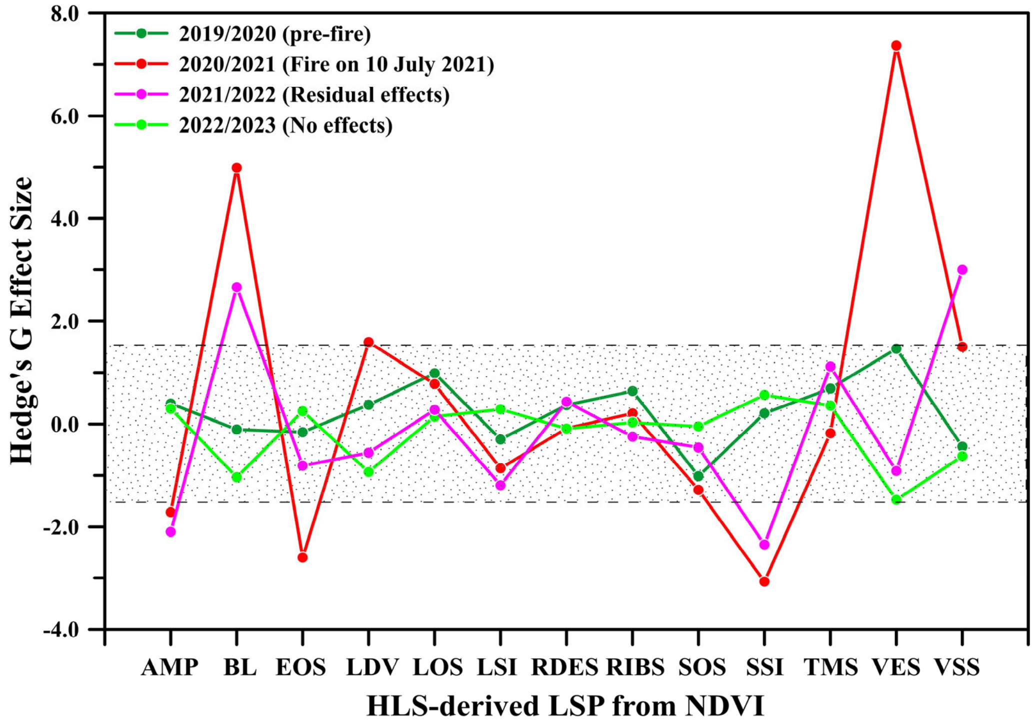

Figure 14. Effect size of fire occurrence starting on 10 July 2021, on HLS-derived Land Surface Phenology (LSP) metrics, calculated from NDVI, for seasonal cycles ranging from 2019/2020 (pre-fire) to 2022/2023. The Hedge's G metric was used to compare adjacent burned and non-burned (control) grassland areas. The burned area influenced the determination of LSP metrics beyond the shaded area, affecting both the seasonal cycle during which the event occurred (2020/2021) and the following cycle (2021/2022). Abbreviations are defined in the text.

To ensure confidence in the data analysis, we plotted the relative frequency distribution of the 500 pixels sampled from both control and burned sites for the NDVI-derived HLS metrics SSI, BL, and VES. Results are shown across the seasonal cycles before the fire (2019/2020), during the fire event (2020/2021), and after the fire (2021/2022 and 2022/2023 cycles) (Figure 15). Confirming the previous MODIS results from Figures 11 and 12, the SSI in burned areas (represented by red histograms in Figure 15) increased compared to control sites (green histograms) in the 2020/2021 and 2021/2022 cycles, while the opposite trend was observed for BL and VES. For each metric, the differences between control and burned sites were small in the pre-fire cycle, as expected, increased during the 2020/2021 (fire occurrence) and 2021/2022 (vegetation recovery) cycles, and decreased again in the 2022/2023 cycle. Metrics like VES exhibited also changes in data variability, as reflected in the altered shape of the histograms (Figure 15).

Finally, confirming the Hedge's G pattern observed for VSS in Figure 14, the spatial distribution of this metric was altered in the fire-affected site compared to the control site (Figure 16). Consistent with our previous results, the most significant changes in VSS occurred during the 2021/2022 cycle, following the major fire event in 2021, as indicated by the shift from green to orange and red colors in the burned area (Figure 16). For the VES (Figure A4 in Appendix A), the most significant effects of the disturbance were observed during the 2020/2021 cycle, aligning with the results (red line) presented in Figure 14. However, a detailed examination of the VES image in Figure A4 revealed residual fire effects in the 2021/2022 cycle for certain pixels within the burned area, though these effects were not substantial enough to impact the Hedge's G metric.

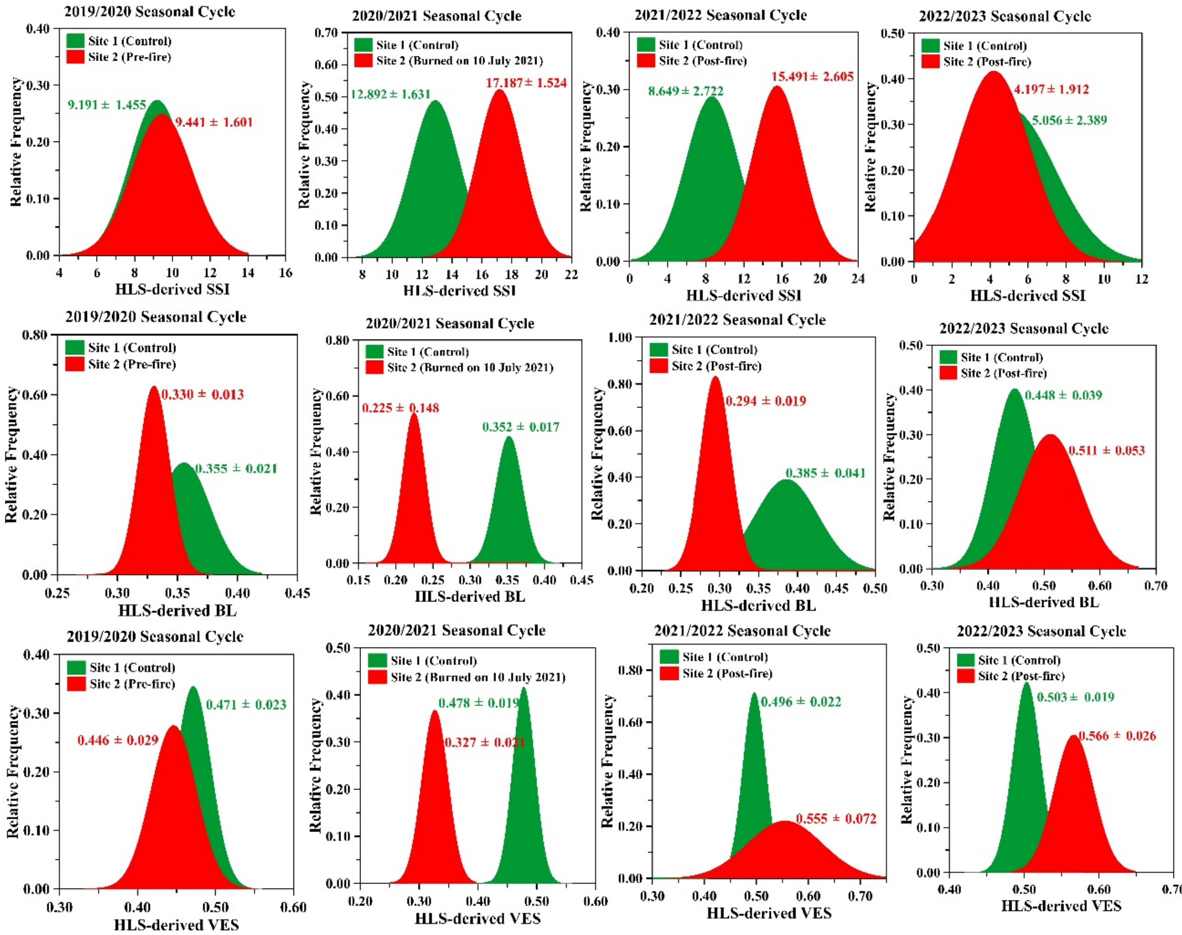

Figure 15. Pairs of Gaussian-fitted histograms for the control (Site 1) and burned (Site 2) grassland sites, illustrating relative variations in the HLS-derived phenological metrics: Small Seasonal Integral (SSI; **top**), Base Level (BL; **middle**), and Value for the End of the Season (VES; **bottom**). Results are presented for the seasonal cycle preceding the fire event (2019/2021), the cycle during which the fire occurred (2020/2021), and two post-fire cycles characterized by vegetation recovery (2021/2022 and 2022/2023).

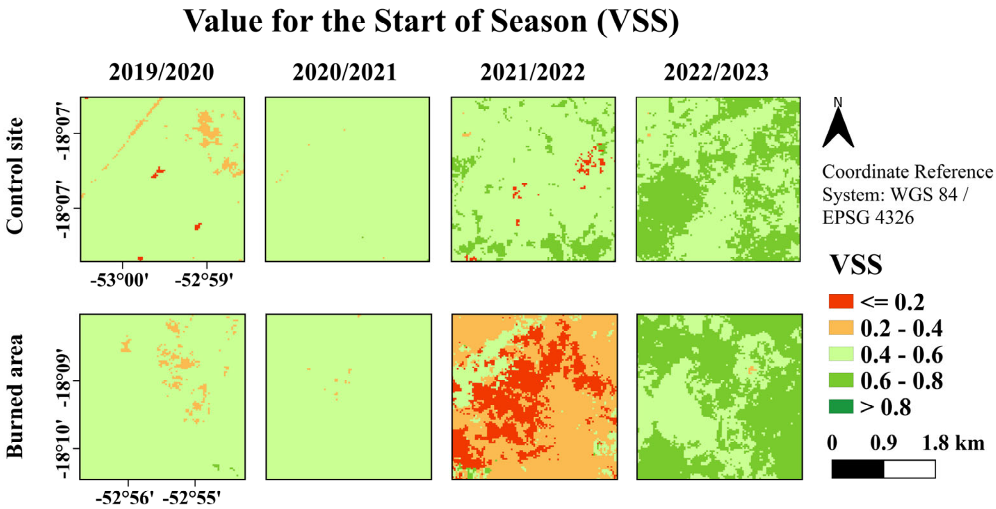

Figure 16. Spatial variation in the Value for the Start of Season (VSS) across control and burned sites, highlighting the effects on the subsequent seasonal cycle following the fire event on 10 July 2021. Results are presented for the seasonal cycle preceding the fire event (2019/2021), the cycle during which the fire occurred (2020/2021), and two post-fire cycles characterized by vegetation recovery (2021/2022 and 2022/2023).

4. Discussion

Our study contributes to the understanding of vegetation phenology in the Brazilian savannas (Cerrado) in several ways. It provides insights into fire-related variability for further long-term trend analyses of satellite-based indicators of vegetation phenology. We found that certain metrics increased in response to both precipitation and fire, with the effects of fire generally being more pronounced than those of precipitation. Given that LSP metrics are often used as input data for classifying savanna vegetation, our findings suggest also that the selection of seasonal cycles influenced by droughts, and consequently by rising fire frequency, can introduce significant variability into the classification results. Our work contributes also to future research employing diverse or more in-depth approaches to better understand savanna dynamics in the face of climate change and fire disturbance. This knowledge is important for developing appropriate conservation strategies in the Brazilian savanna areas.

In the Cerrado, fire is an important ecological element in maintaining its vegetation. However, fire frequency and intensity have been increasing due to climate change, land-use and land-cover changes, and overall human occupation, particularly in the new agricultural frontiers of the Brazilian savannas (e.g., MATOPIBA region) [14,15]. Consequently, there is a reduction of the biome's regeneration capacity, causing loss of woody species. Under predicted scenarios of warmer and drier conditions, the occurrence of fire is expected to spread, making the monitoring of vegetation phenology with satellites essential. Land-degraded areas are projected to increase in the near future, and the recovery of savanna vegetation will vary among woody species.

In our study, fire and vegetation recovery in burned areas introduced data variability into LSP metrics, likely influencing the correlations between phenological metrics and precipitation. The effects were observed during both the cycle in which the disturbance occurred and the post-fire cycle. In this context, the study of the relationships between vegetation phenology and precipitation is important for understanding vegetation productivity, carbon storage, and carbon cycle in terrestrial ecosystems [44]. Distinct responses of savannas to rainfall variability may be also influenced by the ratio of woody to herbaceous biomass. In general, higher woody biomass fractions promote greater stability and resilience to potential scenarios of climate change [50]. In the Brazilian savanna, precipitation and the resultant soil moisture availability are the primary drivers of vegetation structure and diversity [51]. Precipitation, soil moisture conditions, and the availability of dry biomass (fire fuel) are also key factors controlling fire occurrence in the Cerrado biome [11,52].

Our results confirmed that the interannual variations in rainfall had distinct effects on the determination of phenological metrics in grassland and woodland areas of the ENP over the studied seasonal cycles. In grassland areas, MODIS NDVI-derived LSI and SSI were the most sensitive LSP metrics to rainfall during vegetation growing cycles, as evidenced by the positive correlations between accumulated precipitation in the rainy season and these TIMESAT metrics. In woodland areas, AMP, EOS, LSI, RIBS, and SSI also increased in response to seasonal cycles of higher precipitation. Therefore, seasonal cycles of higher precipitation extended the local growing season, increasing vegetation greenness at the start of the season, and enhancing overall NDVI variability and vegetation activity throughout the growing period, as indicated by the behavior of these LSP metrics with increased precipitation. In the literature, these metrics are also important for monitoring other ecosystems. For example, EOS is valuable for evaluating vegetation dynamics in response to severe droughts, while AMP reflects the intensity of vegetation seasonality and its resilience to extreme climatic events. Similarly, BL shows significant variations when vegetation is particularly sensitive to environmental changes [44,53,54]. In agricultural management, SOS, LOS, and EOS are essential for planning planting and harvest periods. Vegetation with higher LSI tends to exhibit greater productivity. When combined with other data, these LSP metrics are also effective for monitoring water or thermal stress in vegetation [29,45,55].

In our study, some MODIS LSP metrics in woodland areas exhibited higher positive correlations with precipitation than those observed in grassland areas. In addition to the difficulties of mapping savanna vegetation physiognomies and the differences in soil composition/texture at the ENP that influence soil water infiltration and water availability to plants, grassland areas have historically been more affected by fire disturbance than woodland areas. Compared to woodland areas, this greater fire disturbance in grassland areas likely contributed to the variability observed in the correlation results presented in Figure 7. For example, a report by França et al. [35] on fire occurrence between 1973 and 2003 at the ENP indicated that the number of repeated fire events in grassland areas ranged from 10 to 18 times, having a lower observed frequency in woodland areas.

Our analysis, based on three major fire events (2005, 2010, and 2021) and utilizing both the MODIS MOD13Q1 and HLS products, highlighted the sensitivity of LSP metrics to fire activity and subsequent vegetation recovery in burned areas. This type of disturbance explains also part of the significant color variability in grasslands observed in the false color composites of Figure 10 for post-fire image acquisition dates. Coupled trend effects of precipitation and fire were observed for metrics such as AMP, EOS, and SSI, which increased with both rainfall and the occurrence of fire. The effects of fire on these metrics were apparently more pronounced than those associated with precipitation, as indicated by a comparative analysis of effect sizes in savanna grasslands (Table A1 in Appendix A). Hedge's G values were higher for fire than for precipitation. Caution is warranted in this analysis due to the use of different remote-sensing products with distinct spatial resolutions and sample locations. In Table A1, Hedge's G values for precipitation were derived from the MOD13Q1 product (n = 500 pixels), based on a comparison between two contrasting seasonal cycles—dry (2006/2007) and wet (2019/2020)—both characterized by minimal fire disturbance. The difference in accumulated rainfall during the rainy season between these two cycles was approximately 550 mm. In contrast, fire-related Hedge's G values were calculated using the HLS product (n = 500 pixels), comparing a burned grassland site with a nearby unburned control site.

By decoupling the effects of fire from rainfall influence using a control site near a burned grassland area, we identified the most sensitive LSP metrics to burning events among the 13 TIMESAT metrics: BL, VES, SSI, VSS, EOS, and AMP. For instance, in the effect's size analysis of the 10 July 2021 fire event (2020/2021 growing cycle) using Hedges' G metric, most of these TIMESAT metrics derived from the HLS product showed high sensitivity to fire events during the cycle in which the disturbance occurred and in the subsequent cycle following disturbance (residual effects due to vegetation recovery in burned areas). The exception was VSS, which marked the beginning of the next growing season. For the 2021 fire event, VSS was primarily influenced by fire effects in the subsequent 2021/2022 cycle, as expected. Among these metrics, AMP, EOS, and SSI increased during the fire-impacted seasonal cycle, while BL, VES, and VSS decreased.

The use of the most sensitive LSP metrics to precipitation and fire detected in our analysis can support also ecosystem management and conservation strategies. For instance, changes in EOS and BL reflect vegetation resilience following disturbances like fires or droughts [53,54]. Persistent alterations in AMP may indicate areas undergoing ecological degradation that should be monitored [44]. When combined with SSI, which indicates vegetation vigor in the season, these metrics can help identify areas with potential for restoration or those requiring prioritization for conservation [45]. Monitoring these metrics in protected areas, such as the ENP, is crucial for guiding adaptive vegetation strategies, including controlled burns and firebreak maintenance.

In the burned grassland site, vegetation recovery began a few days after the fire disturbance that occurred on 10 July 2021 during the local dry season of the 2020/2021 cycle. Vegetation recovery accelerated in October and November 2021 following the first rainfall events of the new seasonal cycle (October 2021 to September 2022), resulting in greener grasses (higher NDVI compared to the control site) from November through the end of the subsequent dry season, extending into September 2022. These results emphasize the superior adaptability of the Cerrado vegetation to fire events, particularly when compared to semi-arid ecosystems, where recovery may take up to two years after a fire due to severe drought conditions [13]. However, when compared to grasslands, the recovery of the structure and floristic composition of burned woody species may take up to eight years, as reported by Machida et al. [56]. In the northern portion of the Cerrado biome, Carvalho et al. [57] noted that areas with higher fire frequencies exhibited slower recovery rates of woody species, with significant effects on phenological metrics like the SOS and EOS.

Our study has some limitations that should be addressed in future investigations. First, we used the MODIS MOD13Q1 vegetation index product, which is provided at 16-day intervals and a 250-m spatial resolution. While this product allows for consistent spatial and temporal comparisons of vegetation canopy greenness, an eight-day composite product would likely be a better alternative for LSP studies of savanna vegetation. However, due to the large field-of-view of MODIS, bidirectional and atmospheric effects resulting from view-illumination geometry during data acquisition could introduce additional uncertainties in the analysis. In reality, a comparison of MODIS-based LSP estimates in Canadian prairie grasslands has shown no significant difference in the phenological metrics derived from daily reference observations and multi-day NDVI resampled at a time step less than 18 days [58]. Second, another limitation is the current version of the TIMESAT software (version 3.3), which is not designed to handle irregular time series of vegetation indices like those produced by the HLS product, demanding data regularization steps. A new version of TIMESAT that can process irregular time-step data is expected to be released for the remote sensing community in the near future. In our study, we used interpolation and gap-filling techniques to overcome this limitation, converting the HLS product into a regularly spaced five-day product with near-nadir viewing. Third, it is important also to note that our analysis of the relationship between precipitation and LSP metrics did not detect severe dry or wet seasonal cycles during the selected period of MODIS observations (2002–2023) when compared to the long-term precipitation measured by the meteorological station (1983–2023). In addition to the influence of burned areas on the results, the absence of severe wet and dry seasonal cycles may have reduced data variability, potentially affecting the magnitude of the observed correlations between phenological metrics and precipitation, which were generally lower than 0.60.

Finally, our approach, which primarily relies on statistical analyses, may not fully capture complex nonlinear relationships with LSP metrics. For instance, interrelated factors such as soil moisture, soil composition, and vegetation type, represented here by two broad classes (grasslands and woodlands), were not examined in detail. According to the literature, vegetation types and plant species composition in the Cerrado biome are largely shaped by a combination of precipitation (i.e., water availability), soil composition, and fire regimes [59]. Soil moisture, in turn, is influenced by soil composition or texture, which affects both fertility and the rate of water infiltration with soil depth. These factors determine the availability of nutrients and water to shallow and deep roots across different vegetation physiognomies. In this context, temperature and topographic relief play a secondary role in the Brazilian savannas. In the Southwest Goiás Microregion, where the

ENP is located in Brazil and surrounded by agricultural land, Silva et al. [60] identified long-term declines in MODIS NDVI, which can influence vegetation phenology. Approximately 50% of these declines, likely associated with land degradation, occurred in pastures converted from savanna vegetation and situated on sandy soils. An additional 25% were observed in native savanna vegetation and 14% in croplands. The ENP itself exhibited overall NDVI stability, with only a few long-term declines detected in the southern portion of the park [59]. This area is characterized by a notably high fire frequency, with over ten fire events recorded solely between 1973 and 2003 [35]. However, the relationships among fire frequency, NDVI declines, and the determination of vegetation phenological metrics require further investigation.

Despite these limitations, the comparison and convergence of vegetation phenology results derived from both products (MOD13Q1 and HLS) at the ENP have provided confidence in the analysis and interpretation of our findings. Vegetation index time series with higher spatial resolution than MODIS are essential for LSP studies of most protected savanna areas in Brazil, given their small size and the challenge of mapping and analyzing them accurately using satellite images. Given the potential importance of phenological metrics in classification studies of savanna physiognomies in protected areas of the Brazilian Cerrado [30–32], it is recommended to select the seasonal cycles least affected by fire disturbance in order to reduce uncertainties in the data analysis and improve classification accuracy. It is also essential to consider fire as a significant factor influencing variability in long-term analyses of phenological metrics, particularly in relation to interannual changes in precipitation.

5. Conclusions

By assessing the effects of precipitation and fire on NDVI-derived phenological metrics at the ENP using the MODIS MOD13Q1 and HLS products, we concluded that the LSP metrics most positively correlated to precipitation were AMP, EOS, LSI, RIBS, and SSI. Similar trend effects of precipitation and fire were observed for AMP, EOS, and SSI, which increased during seasonal cycles with higher precipitation or with greater occurrence of fire activities. Fire effects were more pronounced than those of precipitation. When decoupling the effects of fire from rainfall influence using a control site near a burned grassland area, the metrics most sensitive to fire and subsequent vegetation recovery in burned areas were BL, VES, SSI, VSS, EOS, and AMP.

Based on the specific objectives of this study, the following conclusions were drawn:

(i) We did not detect in our analysis severe dry or wet seasonal cycles in the studied period (2002 to 2023), compared to the long-term rainfall measurements (1983 to 2023). Dry, regular, and wet cycles occurred alternately during the period of satellite observation.

(ii) For the MODIS LSP metrics most sensitive to precipitation, the highest correlation coefficients were observed in woodland areas. This may reflect the higher occurrence of fire disturbance typically observed in grassland areas, which introduces variability into the data analysis.

(iii) Analysis of the three major fire events at the ENP (2005, 2010, and 2021) revealed that the effects of fire were evident during the cycle in which the disturbance occurred, as well as in the subsequent cycle, due to vegetation recovery in fire-affected areas. Compared to control sites, burned areas exhibited greener grasslands, resulting in comparatively higher NDVI values throughout the entire seasonal cycle following the fire.

Author Contributions: Conceptualization and supervision, L.S.G. and T.S.K.; writing and formal analysis, M.C.d.R.S. and L.S.G.; writing—review and editing, T.S.K. and G.R. All authors have read and agreed to the published version of the manuscript.

Funding: This research was funded by the Coordenação de Aperfeiçoamento de Pessoal de Nível Superior (CAPES) (Financial Code 001).

Data Availability Statement: The raw data supporting the conclusions of this article will be made available by the authors on request.

Acknowledgments: The authors are grateful to the Conselho Nacional de Desenvolvimento Científico e Tecnológico (CNPq) (grant numbers 307792/2021-8 and 302205/2023-3) and Fundação de Amparo à Pesquisa do Estado de São Paulo (FAPESP) (grant number 2023/09118-6). Comments by three anonymous reviewers were highly appreciated.

Conflicts of Interest: The authors declare no conflicts of interest.

Appendix A

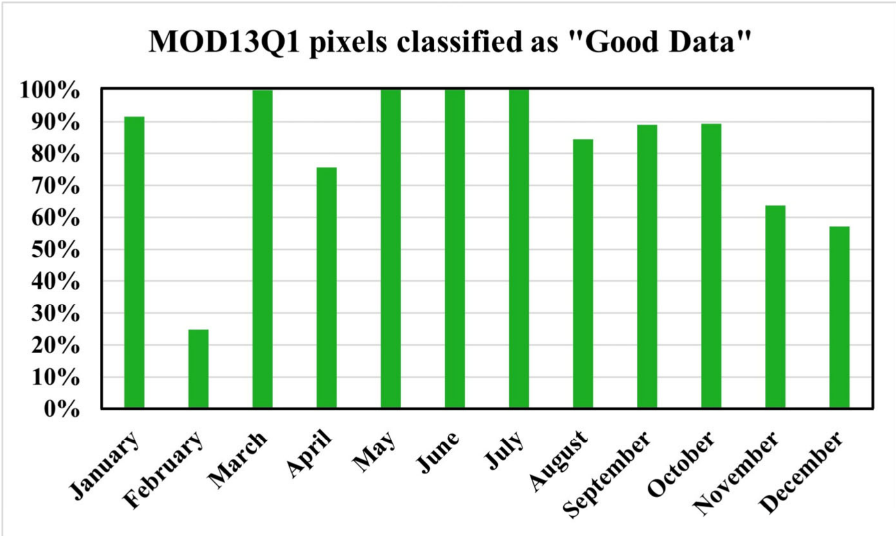

Figure A1. Intra-annual variations in Good Quality pixels (code 0 in the pixel reliability dataset) from the MODIS MOD13Q1 product during the local rainy season (October to May) and the dry season (June to September). Data refer to 2019.

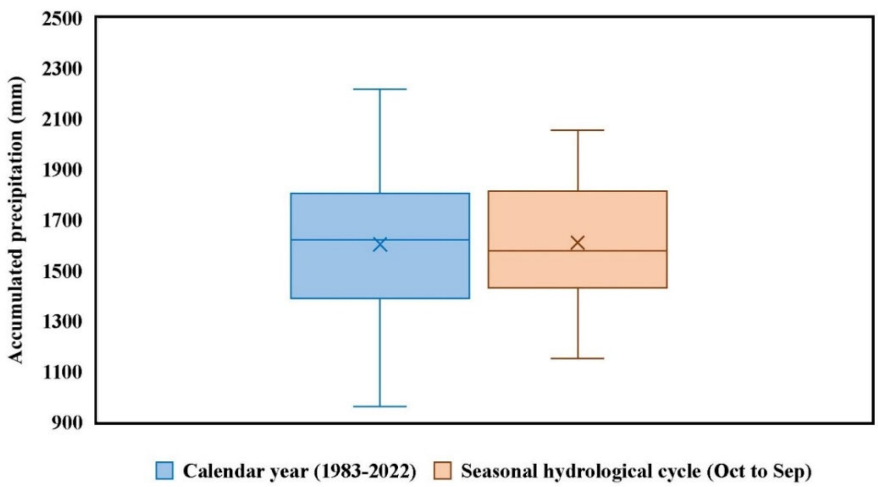

Figure A2. Interannual variations in accumulated precipitation during the seasonal cycles of MODIS data acquisition (2002/2003 to 2022/2023) at Emas National Park (ENP), compared to the long-term period from 1983 to 2022. Each seasonal cycle spans from October to September of the following year. The mean (crosses), median (horizontal lines within boxes), and standard deviation bars are displayed.

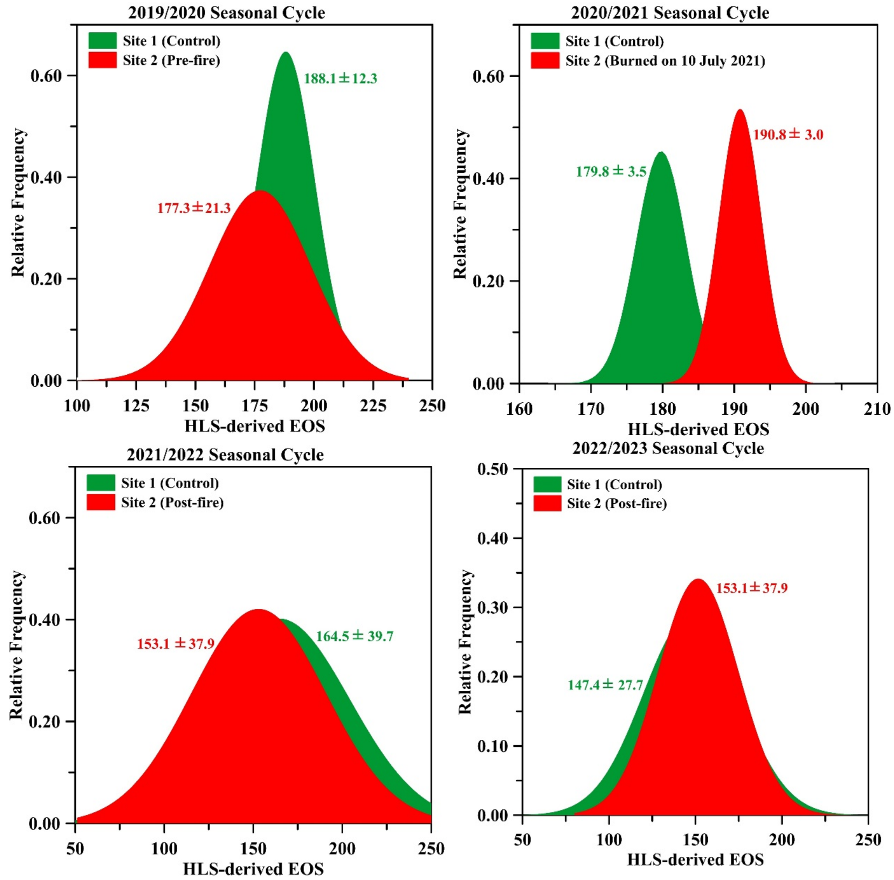

Figure A3. Pairs of Gaussian-fitted histograms for the control (Site 1) and burned (Site 2) grassland sites, illustrating relative variations in the HLS-derived phenological metric End of Season (EOS). Results are presented for the seasonal cycle preceding the fire event (2019/2021), the cycle during which the fire occurred (2020/2021), and two post-fire cycles characterized by vegetation recovery (2021/2022 and 2022/2023).

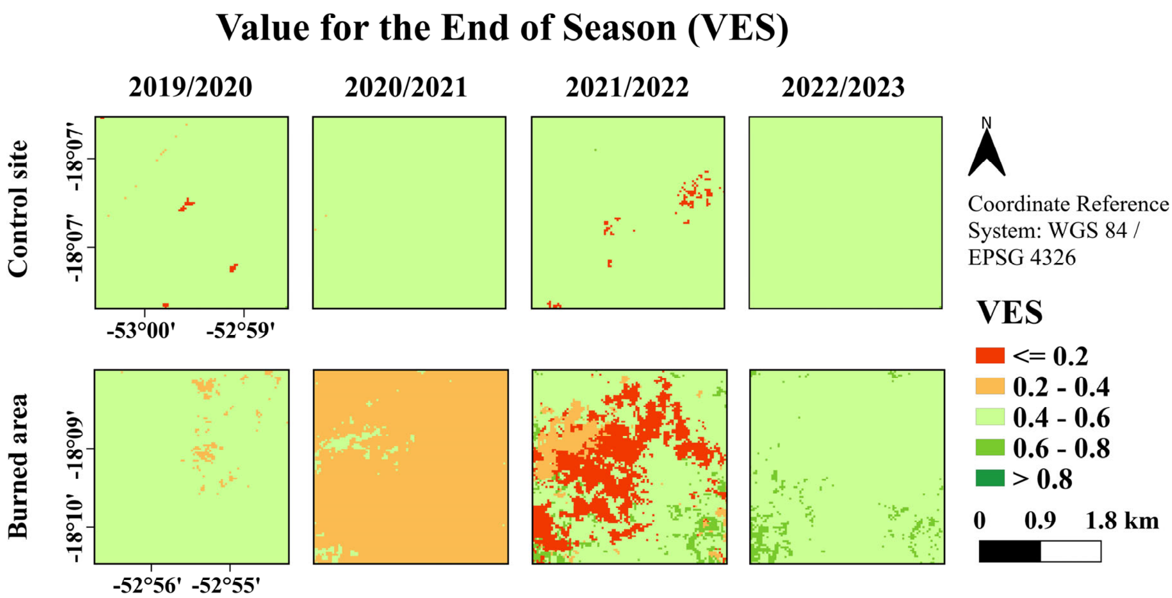

Figure A4. Spatial variation in the Value for the End of Season (VES) across control and burned sites, highlighting the effects on the subsequent seasonal cycle following the fire event on 10 July 2021. Results are presented for the seasonal cycle preceding the fire event (2019/2021), the cycle during which the fire occurred (2020/2021), and two post-fire cycles characterized by vegetation recovery (2021/2022 and 2022/2023).

Table A1. Comparative analysis of precipitation and fire effect sizes (Hedge's G) on Amplitude (AMP), End of Season (EOS), and Small Seasonal Integral (SSI) in savanna grasslands of the Emas National Park (ENP). Hedge's G values for precipitation were derived from the MOD13Q1 product (n = 500 pixels), comparing contrasting seasonal cycles—dry (2006/2007) and wet (2019/2020)—with minimal fire disturbance. Fire-related Hedge's G values were calculated using the HLS product (n = 500 pixels), comparing a burned grassland site with an adjacent unburned control site.

Vegetation Phenological Metric	Precipitation (Dry Versus Wet Cycle) MOD13Q1 Product	Fire (Burned Versus Non-Burned) HLS Product
AMP	−0.402	−2.096
EOS	−0.037	−2.599
SSI	−1.330	−3.072

References

1. Ferreira, L.G.; Asner, G.P.; Kanapp, D.E.; Coe, M.; Bustamante, M.M.C.; Oliveira, E.L. Equivalent water thickness in savanna ecosystems: MODIS estimates based on ground and EO-1 Hyperion data. *Int. J. Remote Sens.* **2011**, *32*, 7423–7440. [CrossRef]
2. Sano, E.E.; Rosa, R.; Scaramuzza, C.A.M.; Adami, M.; Bolfe, E.L.; Coutinho, A.C.; Esquerdo, J.C.D.M.; Maurano, L.E.P.; Narvaes, I.d.S.; Filho, F.J.B.d.O.; et al. Land use dynamics in the Brazilian Cerrado in the period from 2002 to 2013. *Pesqui. Agropecuária Bras.* **2019**, *54*, e00138. [CrossRef]
3. Jacon, A.D.; Galvão, L.S.; Santos, J.R.; Sano, E.E. Seasonal characterization and discrimination of savannah physiognomies in Brazil using hyperspectral metrics from Hyperion/EO-1. *Int. J. Remote Sens.* **2017**, *38*, 4494–4516. [CrossRef]
4. Ribeiro, J.F.; Walter, B.M.T. Fitofisionomias do bioma Cerrado. In *Cerrado: Ambiente e flora*; Sano, S.M., Almeida, S.P., Eds.; Embrapa-CPAC: Brasília, Brazil, 1998; 556p.
5. Oliveira-Filho, A.T.; Ratter, J.A. Vegetation physiognomies and woody flora of the Cerrado biome. In *The Cerrados of Brazil*; Oliveira, P.S., Marquis, R.J., Eds.; Columbia University Press: New York, NY, USA, 2002; pp. 91–120. [CrossRef]
6. Araújo, J.A.; Galvão, L.S.; Dalagnol, R. Sensitivity of hyperspectral vegetation indices to rainfall seasonality in the Brazilian savannahs: An analysis using PRISMA data. *Remote Sens. Lett.* **2023**, *14*, 277–287. [CrossRef]
7. Kraaij, T.; Cowling, R.M.; van Wilgen, B.W.; Rikhotso, D.R.; Difford, M. Vegetation responses to season of fire in a seasonal, fire-prone fynbos shrubland. *PeerJ* **2017**, *5*, e3591. [CrossRef]
8. Currier, C.M.; Sala, O.E. Precipitation versus Temperature as Phenology Controls in Drylands. *Ecology* **2022**, *103*, e3793. [CrossRef] [PubMed]
9. Lu, C.; Zhang, J.; Min, X.; Chen, J.; Huang, Y.; Zhao, H.; Yan, T.; Liu, X.; Wang, H.; Liu, H. Contrasting responses of early- and late-season plant phenophases to altered precipitation. *Oikos* **2023**, *5*, e09829. [CrossRef]
10. Bond, W.J.; Woodward, F.I.; Midgley, G.F. The global distribution of ecosystems in a world without fire. *New Phytol.* **2005**, *165*, 525–538. [CrossRef] [PubMed]
11. Alvarado, S.T.; Fornazari, T.; Cóstola, A.; Morellato, L.P.C.; Silva, T.S.F. Drivers of fire occurrence in a mountainous Brazilian cerrado savanna: Tracking long-term fire regimes using remote sensing. *Ecol. Indic.* **2017**, *78*, 270–281. [CrossRef]
12. Silva, L.S.; Costa, T.R.; Salomão, N.V.; Otoni, T.J.O.; Machado, E.L.M. After-fire Variations in Floristic Composition at the Cerrado (Brazilian Savannah) Phytophysiognomies in Curvelo, Minas Gerais, Brazil. *Floresta E Ambiente* **2020**, *27*, e20180188. [CrossRef]
13. Karimi, S.; Heydari, M.; Mirzael, J.; Karami, O.; Heung, B.; Mosavi, A. Assessment of Post-Fire Phenological Changes Using MODIS-Derived Vegetative Indices in the Semiarid Oak Forests. *Forests* **2023**, *14*, 590. [CrossRef]
14. Enright, N.J.; Fontaine, J.B.; Bowman, D.M.J.S.; Bradstock, R.A.; Williams, R.J. Interval squeeze: Altered fire regimes and demographic responses interact to threaten woody species persistence as climate changes. *Front. Ecol. Environ.* **2015**, *13*, 265–272. [CrossRef]
15. Gomes, L.; Miranda, H.S.; Soares-Filho, B.; Rodrigues, L.; Oliveira, U.; Bustamante, M.M.C. Responses of Plant Biomass in the Brazilian Savanna to Frequent Fires. *Front. For. Glob. Chang* **2020**, *3*, 507710. [CrossRef]
16. Silvério, D.V.; Pereira, O.R.; Mews, H.A.; Maracahipes-Santos, L.; dos Santos, J.O.; Lenza, E. Surface fire drives short-term changes in the vegetative phenology of woody species in a Brazilian savanna. *Biota Neotrop.* **2015**, *15*, e20140077. [CrossRef]
17. Geng, L.; Che, T.; Wang, X.; Wang, H. Detecting Spatiotemporal Changes in Vegetation with the BFAST Model in the Qilian Mountain Region during 2000–2017. *Remote Sens.* **2019**, *11*, 103. [CrossRef]
18. Ibrahim, S.; Kaduk, J.; Tansey, K.; Balzter, H.; Lawal, U.M. Detecting phenological changes in plant functional types over West African savannah dominated landscape. *Int. J. Remote Sens.* **2021**, *42*, 567–594. [CrossRef]

19. Borges, E.F.; Sano, E.E. Temporal series of EVI from MODIS sensor for land use and land cover mapping of western Bahia. *Bol. De Ciências Geodésicas* **2014**, *20*, 526–547. [CrossRef]
20. Saad, S.I.; Rocha, H.R.; Dias, M.A.F.S.; Rosolem, R. Can the deforestation breeze change the rainfall in Amazonia? A case study for the BR-163 highway region. *Earth Interact.* **2010**, *14*, 1–25. [CrossRef]
21. Chai, Y.; Martins, G.; Nobre, C.; von Randow, C.; Chen, T.; Dolman, H. Constraining Amazonian land surface temperature sensitivity to precipitation and the probability of forest dieback. *Clim. Atmos. Sci.* **2021**, *4*, 6. [CrossRef]
22. Pennington, R.T.; Lehmann, C.E.R.; Rowland, L.M. Tropical savannas and dry forests. *Curr. Biol.* **2018**, *28*, 527–548. [CrossRef]
23. Ma, X.; Jin, J.; Zhu, X.; Zhou, Y.; Xie, Q. Remote Sensing of Land Surface Phenology: Editorial. *Remote Sens.* **2022**, *14*, 4310. [CrossRef]
24. Gao, X.; McGregor, I.R.; Gray, J.M.; Friedl, M.A.; Moon, M. Observations of satellite land surface phenology indicate that maximum leaf greenness is more associated with global vegetation productivity than growing season length. *Glob. Biogeochem. Cycles* **2023**, *37*, e2022GB007462. [CrossRef]
25. Li, Z.; Shi, H.; Vogelmann, J.E.; Hawbaker, T.J.; Peterson, B. Assessment of Fire Fuel Load Dynamics in Shrubland Ecosystems in the Western United States Using MODIS Products. *Remote Sens.* **2020**, *12*, 1911. [CrossRef]
26. Didan, K.; Munhoz, A.B. MODIS Vegetation Index User's Guide (MOD13 Series) Version 3.10, 2019 (Collection 6.1). The University of Arizona. Available online: https://vip.arizona.edu (accessed on 13 April 2025).
27. Eklundh, L.; Jonsson, P. *TIMESAT 3.3 Software Manual*; Lund and Malmö University: Scandinavia, Sweden, 2017.
28. Dronova, I.; Taddeo, S. Remote sensing of phenology: Towards the comprehensive indicators of plant community dynamics from species to regional scales. *J. Ecol.* **2022**, *110*, 1460–1484. [CrossRef]
29. Rodigheri, G.; Sanches, I.D.; Richetti, J.; Tsukahara, R.Y.; Lawes, R.; Bendini, H.N.; Adami, M. Estimating Crop Sowing and Harvesting Dates Using Satellite Vegetation Index: A Comparative Analysis. *Remote Sens.* **2023**, *15*, 5366. [CrossRef]
30. Schwieder, M.; Leitão, P.J.; Bustamante, M.M.C.; Ferreira, L.G.; Rabe, A.; Hostert, P. Mapping Brazilian savanna vegetation gradients with Landsat time series. *Int. J. Appl. Earth Obs. Geoinf.* **2016**, *52*, 361–370. [CrossRef]
31. Haddad, I.; Galvão, L.S.; Breunig, F.M.; Dalagnol, R.; Bourscheidt, V.; Jacon, A.D. On the combined use of phenological metrics derived from different Planetscope vegetation indices for classifying savannas in Brazil. *Remote Sens. Appl. Soc. Environ.* **2022**, *26*, 100764. [CrossRef]
32. Araújo, J.A.; Galvão, L.S.; Dalagnol, R. Evaluating changes with vegetation cover in PRISMA's spectral, spatial, and temporal attributes and their performance for classifying savannahs in Brazil. *Remote Sens. Appl. Soc. Environ.* **2023**, *32*, 101074. [CrossRef]
33. Masek, J.; Ju, J.; Roger, J.; Skakun, S.; Vermote, E.; Claverie, M.; Dungan, J.; Yin, Z.; Freitag, B.; Justice, C. HLS Sentinel-2 MSI Surface Reflectance Daily Global 30 m V1.5. NASA EOSDIS Land Processes Distributed Active Archive Center 2020. Available online: https://lpdaac.usgs.gov/products/hlss30v015/ (accessed on 14 April 2025).
34. Ju, J.; Neigh, C.; Claverie, M.; Skakun, S.; Roger, J.C.; Vermote, E.; Dungan, J. Harmonized Landsat Sentinel-2 (HLS). In *Product User Guide: Product Version 2.0*; National Aeronautics and Space Administration (NASA): Washington, DC, USA, 2023; 23p.
35. França, H.; Ramos Neto, M.B.; Setzer, A. *O fogo no Parque Nacional das Emas (Série Biodiversidade)*; Ministério do Meio Ambiente: Brasília, Brazil, 2007; Volume 27, 140p.
36. Batista, F.R.Q. Manejo e Monitoramento de Impactos Sobre o Ecossistema em Áreas Protegidas de Cerrado: Estrutura da Vegetação, Gramíneas Exóticas e Incêndios. Ph.D. Thesis, Universidade Federal de Goiás, Goiânia, Brazil, 2019; 165p.
37. Ramos-Neto, M.B. O Parque Nacional das Emas (GO) e o fogo: Implicações para a conservação biológica. Ph.D. Thesis, Instituto de Biociências, Universidade de São Paulo, São Paulo, Brazil, 2000; 159p.
38. Rouse, J.W.; Haas, R.H.; Schell, J.A.; Deering, D.W. Monitoring Vegetation Systems in the Great Plains with ERTS. In Proceedings of the Third ERTS-1 Symposium, Washington, DC, USA, 10–14 December 1973; NASA SP-351. Volume 1, pp. 309–317.
39. Matsushita, B.; Yang, W.; Chen, J.; Onda, Y.; Qiu, G. Sensitivity of the Enhanced Vegetation Index (EVI) and Normalized Difference Vegetation Index (NDVI) to Topographic Effects: A Case Study in High-Density Cypress Forest. *Sensors* **2007**, *7*, 2636–2651. [CrossRef]
40. Oliveira, L.M.; Galvão, L.S.; Ponzoni, F.J. Topographic Effects on the Determination of Hyperspectral Vegetation Indices: A Case Study in Southeastern Brazil. *Geocarto Int.* **2021**, *36*, 2186–2203. [CrossRef]
41. Galvão, L.S.; Arlanche Petri, C.; Dalagnol, R. Coupled effects of solar illumination and phenology on vegetation index determination: An analysis over the Amazonian forests using the SuperDove satellite constellation. *GIScience Remote Sens.* **2024**, *61*, 2290354. [CrossRef]
42. Jonsson, P.; Eklundh, L. TIMESAT—A program for analysing time-series of satellite sensor data. *Comput. Geosci.* **2004**, *8*, 833–845. [CrossRef]
43. Lara, B.; Gandini, M. Assessing the performance of smoothing functions to estimate land surface phenology on temperate grassland. *Int. J. Remote Sens.* **2016**, *37*, 1801–1813. [CrossRef]
44. Zheng, W.; Liu, Y.; Yang, X.; Fand, W. Spatiotemporal Variations of Forest Vegetation Phenology, and Its Response to Climate Change in Northeast China. *Remote Sens.* **2022**, *14*, 2909. [CrossRef]

45. Alemayehu, B.; Suarez-Minguez, J.; Rosette, J.; Khan, S.A. Vegetation Trend Detection Using Time Series Satellite Data as Ecosystem Condition Indicators for Analysis in the Northwestern Highlands of Ethiopia. *Remote Sens.* **2023**, *15*, 5032. [CrossRef]
46. Bendini, H.N.; Fonseca, L.M.G.; Schwieder, M.; Korting, T.S.; Ruffin, P.; Sanches, I.D. Comparing Phenometrics Extracted from Dense Landsat-Like Image Time Series for Crop Classification. In Proceedings of the IEEE International Geoscience and Remote Sensing Symposium, Yokohama, Japan, 28 July–2 August 2019. [CrossRef]
47. Caparros-Santiago, J.A.; Rodriguez-Galiano, V.; Dash, J. Land surface phenology as indicator of global terrestrial ecosystem dynamics: A systematic review. *ISPRS J. Photogramm. Remote Sens.* **2021**, *171*, 330–347. [CrossRef]
48. Galvani, E.; Luchiari, A. Critérios para classificação de anos com regime pluviométrico normal, seco e úmido. In Proceedings of the Anais do X Encontro de Geógrafos da América Latina, São Paulo, SP, Brazil, 20–26 March 2005; pp. 5701–5710.
49. Lakens, D. Calculating and reporting effect sizes to facilitate cumulative science: A practical primer for *t*-tests and ANOVAs. *Front. Psychol.* **2013**, *4*, 863. [CrossRef] [PubMed]
50. Ma, X.; Huete, A.; Yu, Q.; Coupe, N.R.; Davies, K.; Broich, M.; Ratana, P.; Beringer, J.; Hutley, L.B.; Cleverly, J.; et al. Spatial patterns and temporal dynamics in savanna vegetation phenology across the North Australian Tropical Transect. *Remote Sens. Environ.* **2013**, *139*, 97–115. [CrossRef]
51. Lehmann, C.E.R.; Anderson, T.M.; Sankaran, M.; Higgins, S.I.; Archibald, S.; Hoffmann, W.A.; Hanan, N.P.; Williams, R.J.; Fensham, R.J.; Felfili, J.; et al. Savanna vegetation-fire-climate relationships differ among continents. *Science* **2014**, *343*, 548–552. [CrossRef]
52. Krawchuk, M.A.; Moritz, M.A. Constraints on global fire activity vary across a resource gradient. *Ecology* **2011**, *92*, 121–132. [CrossRef]
53. Ge, C.; Sun, S.; Yao, R.; Sun, P.; Li, M.; Bian, Y. Long-term vegetation phenology changes and response to multi-scale meteorological drought on the Loess Plateau, China. *J. Hydrol.* **2022**, *614*, 128605. [CrossRef]
54. Medeiros, R.; Andrade, J.; Ramos, D.; Moura, M.; Pérez-Marin, A.M.; dos Santos, C.A.C.; da Silva, B.B.; Cunha, J. Remote Sensing Phenology of the Brazilian Caatinga and Its Environmental Drivers. *Remote Sens.* **2022**, *14*, 2637. [CrossRef]
55. Singh, R.; Patel, N.R.; Danodia, A. Deriving Phenological Metrics from Landsat-OLI for Sugarcane Crop Type Mapping: A Case Study in North India. *J. Indian Soc. Remote Sens.* **2022**, *50*, 1021–1030. [CrossRef]
56. Machida, W.S.; Gomes, L.; Moser, P.; Castro, I.B.; Miranda, S.C.; Silva-Júnior, M.C.; Bustamante, M.M.C. Long term post-fire recovery of woody plants in savannas of central Brazil. *For. Ecol. Manag.* **2021**, *493*, 119255. [CrossRef]
57. Carvalho, I.S.; Barros, K.A.L.; Alves, D.B.; Ferraz, T.M.; Alvarado, S.T. Relações entre Incidência de Queimadas e a Dinâmica da Vegetação no Parque Nacional da Chapada das Mesas, Maranhão, Brasil: Uma Abordagem a partir de Métricas Fenológicas derivadas de Sensoriamento Remoto. *Rev. Geográfica Acadêmica* **2024**, *18*, 19–41. Available online: https://revista.ufrr.br/rga/article/view/8276 (accessed on 23 March 2025).
58. Cui, T.; Martz, L.; Zhao, L.; Guo, X. Investigating the impact of the temporal resolution of MODIS data on measured phenology in the prairie grasslands. *GIScience Remote Sens.* **2020**, *57*, 395–410. [CrossRef]
59. Bueno, L.M.; Dexter, K.G.; Pennington, R.T.; Pontara, V.; Neves, D.M.; Ratter, J.A.; de Oliveira-Filho, A.T. The Environmental Triangle of the Cerrado Domain: Ecological Factors Driving Shifts in Tree Species Composition between Forests and Savannas. *J. Ecol.* **2018**, *106*, 2109–2120. [CrossRef]
60. Silva, Y.B.A.; Galvão, L.S.; Sanches, I.D.; Oliveira, L.B. On the occurrence and causes of long-term declines in MODIS NDVI within the savanna environment of central Brazil. *Remote Sens. Appl. Soc. Environ.* **2025**, *38*, 101558. [CrossRef]